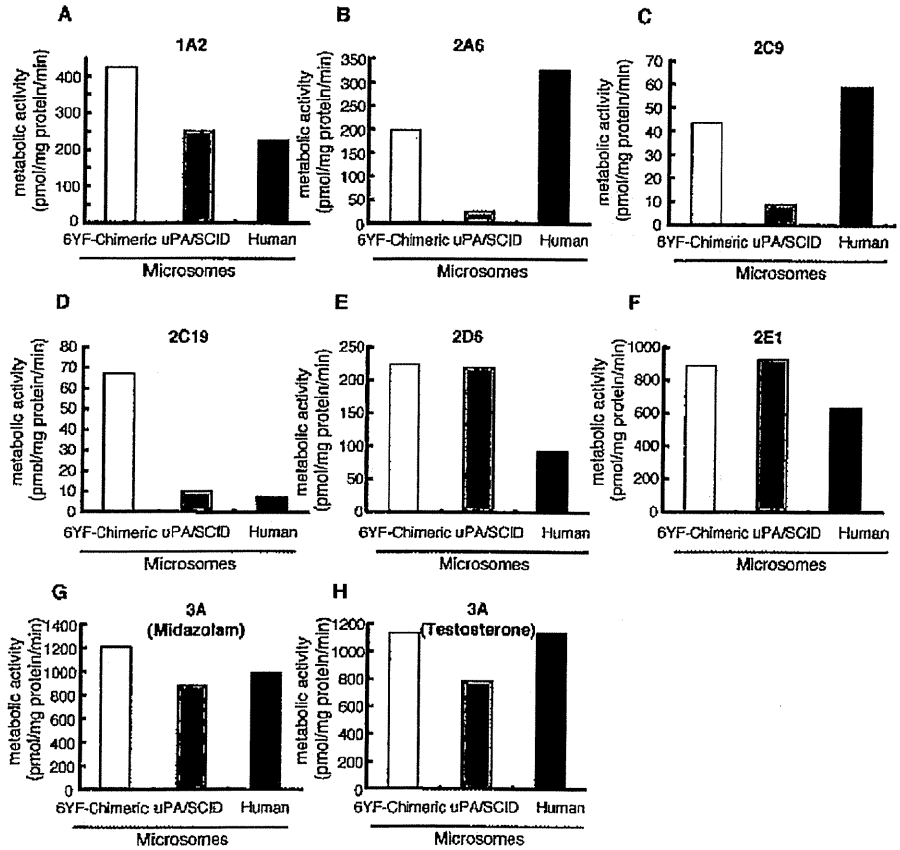

Fig. 3. P450 activities of liver microsomes from chimeric mice, uPA/SCID mice, and human livers as determined by LC-MS/MS Microsomes from a 6YF-chimeric mouse and pooled microsomes of uPA/SCID mice and human livers were treated with eight substrates specific for seven P450s (Table 1), and the metabolite concentrations were measured by LC-MS/MS; the metabolic activity of each P450 is shown as pmol/mg protein/min (Table 2): (A) 1A2, (B) 2A6, (C) 2C9, (D) 2C19, (E) 2D6, (F) 2E1, (G) 3A, midazolam, and (H) 3A, testosterone.

control mice.[13] These findings demonstrate that h-hepatocytes in the chimeric mouse liver had normal human phase I and II enzyme activity, and that the chimeric mice may have advantages in studies of ADME and drug interactions. However, no study had examined the metabolic activity of fresh h-hepatocytes isolated from chimeric mice. In the present study, we determined whether the chimeric mouse could be a useful source of fresh h-hepatocytes for *in vitro* metabolic studies.

The metabolic capacities of fresh and corresponding cryopreserved hepatocytes from several donors have been compared by testosterone hydroxylation, 7-ethoxyresorufin-*O*-deethylase (EROD), and 7-ethoxycoumarin-*O*-deethylase (ECOD). These activities were found to be lower in cryopreserved hepatocytes than in fresh ones.[17,18] Phase II enzyme activities, GST, UGT toward 4-methylumbelliferone (MUF), and sulfotransferase (SULT) were also significantly reduced after cryopreservation of h-hepatocytes, whereas the activity of UGT toward 4-hydroxybiphenyl (HOBI) and that of SULT were similar to those measured in fresh h-hepatocytes.[17] Despite the observed reductions of these enzyme activities, cryopreserved h-hepatocytes are regarded as the best *in vitro* model for use in predicting human intrinsic clearance of xenobiotics.[19] This is because ahead-of-time experimental planning using fresh h-hepatocytes and attaining reproducible studies using the same donor of fresh h-hepatocytes is not feasible. Additionally, because large individual variations are known to exist among h-hepatocytes, pooled hepatocytes derived from several donors could help eliminate such individual variation, but such pooling of fresh h-hepatocytes is not possible. Here, we compared the P450 activities of fresh and cryopreserved chimeric hepatocytes originating from the same donor, and fresh h-hepatocytes from human livers. Results indicated that CYP1A2, 2C19, and 2D6 activities declined, while CYP2A6, 2C9, 2E1, and 3A activities were not affected by the freeze-thaw procedure. Fresh and cryopreserved chimeric h-hepatocytes were used for the determination of ketoprofen glucuronidation. Concentrations of ketoprofen-glucuronide and transferred ketoprofen-glucuronide were higher in fresh chimeric hepatocytes than in their cryopreserved counterparts. Chimeric hepatocytes from the same donor showed

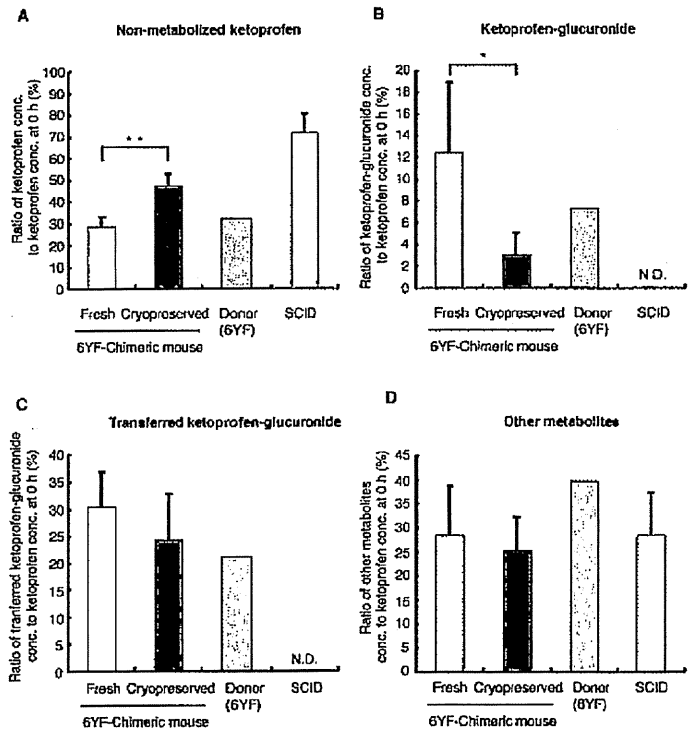

Fig. 4. Glucuronidation of ketoprofen in fresh and cryopreserved chimeric hepatocytes, uPA(wt/wt)/SCID mouse hepatocytes, and cryopreserved donor hepatocytes, as determined by LC-MS/MS

Fresh and cryopreserved chimeric hepatocytes, uPA(wt/wt)/SCID mouse hepatocytes, and cryopreserved donor hepatocytes (6YF) were incubated with ketoprofen for 3 h. The conditioned medium was treated with β-glucuronidase and 1 N KOH, and the concentration of ketoprofen was measured by LC-MS/MS (Table 2): (A) Non-metabolized ketoprofen, (B) Ketoprofen-glucuronide, (C) Transferred ketoprofen-glucuronide, and (D) other metabolites. The concentrations of ketoprofen-glucuronide and transferred ketoprofen-glucuronide were calculated by the formulas indicated in Materials and Methods, and the activities were expressed as the ratio of the concentration of ketoprofen or its glucuronide conjugate to the ketoprofen concentration at 0 h. The values shown are the means ± SD of three or five different chimeric mice. $^{*}p<0.05$, $^{**}p<0.01$. ND, not detected.

smaller variations in P450 activities than fresh h-hepatocytes from different individuals (**Fig. 1**). These results indicated that fresh chimeric hepatocytes may address the problem of individual differences in fresh h-hepatocytes. Additionally, the fresh and cryopreserved chimeric hepatocytes tested retained P450 (CYP1A2, 2C9, 2C19, and 3A) activities for at least 6 h. These studies demonstrated that chimeric mice can provide fresh h-hepatocytes ahead of time, making reproducible studies using the same donor possible.

The decreased metabolism in cryopreserved hepatocytes could be attributable to two mechanisms: inactivation of P450 enzymes and loss of the cofactor NADPH due to cell membrane damage.[20] The addition of a NADPH-generating system to the incubation mixture has been shown to increase benzo[a]pyrene metabolite formation by cryopreserved rat hepatocytes to approximately the level of freshly isolated rat hepatocytes.[21] When cryopreserved rat hepatocytes were purified by Percoll centrifugation after thawing, to remove dead and membrane-damaged cells, benzo[a]pyrene metabolism recovered to equal that of fresh rat hepatocytes.[21] The decline in phase II enzyme activities has also been shown to be overcome by Percoll centrifugation, but not completely to the level of freshly isolated cells.[21] Addition of endogenous cofactors uridine 5′-diphosphoglucuronic acid (UDPGA) and adenosine 3′-phosphate 5′-phosphosulfate (PAPS) to cryopreserved rat hepatocytes improved 7-hydroxycoumarin-glucuronide and 7-hydroxycoumarin-sulfate formation to levels observed in fresh hepatocytes.[22] The UDPGA and PAPS synthesis machineries may be damaged during freezing and thawing. Fresh or cryopreserved chimeric hepatocytes would be useful in clarifying the mechanisms underlying the decline in metabolic activities after freezing and thawing. The results of this study also suggest that fresh chimeric hepatocytes are useful for testing phase I and II reactions, including glucuronidation, without the need for Percoll purification or the addition of cofactors.

Chimeric hepatocytes contain about 17% of m-hepatocytes, and 66Z antibodies react specifically with m-hepatocytes. We purified h-hepatocytes from the chimer-

ic hepatocytes by 66Z rat IgG and magnetic bead-conjugated anti-rat IgG antibodies. After the magnetic removal of m-hepatocytes, the proportion of m-hepatocytes decreased to approximately 3%. We measured the P450 activities of microsomes isolated from the chimeric mouse and pooled microsomes from uPA/SCID mice and human livers using the same substrates as those used in the cell suspension study. Because we were not able to obtain microsomes from the donor of the chimeric mice (6YF), pooled human microsomes were used for this study. Except for CYP2D6 and 2E1, the activities of uPA/SCID mouse liver microsomes were similar to, or lower than, those of pooled human liver microsomes. The activities of CYP2D6 and 2E1 in uPA/SCID mouse liver microsomes were 50–100% higher than those of pooled human liver microsomes, respectively. We also found that P450 activities were similar between pre- and post-purified chimeric hepatocytes. From these results, we deduced that m-hepatocytes contaminating the chimeric hepatocytes might not significantly affect the activities of chimeric hepatocytes.

Gender differences in CYP3A4 activities have been reported when using cryopreserved human hepatocytes.[23] We assumed that P450 activities were independent of the gender in recipient uPA/SCID mice, because we recently showed that there was no significant difference in P450 activity (CYP1A2, 2C9. 2C19, 2D6, and 3A) between microsomes from male and female chimeric mice.[24] In the present study, hepatocytes isolated from both male and female chimeric mice were used, and there was no difference in P450 or UGT activity between them (data not shown); however, the number of animals was limited.

Non-platable 4YF- and 6YF-donor cells were engrafted and grown in the uPA/SCID mice and hepatocytes were isolated from the livers using the collagenase perfusion method. Fresh chimeric hepatocytes adhered well onto the culture dishes, compared with fresh and cryopreserved h-hepatocytes. This suggests that fresh chimeric hepatocytes would be suitable for P450 induction and toxicity studies that are usually performed with plated cells.

Cryopreserved h-hepatocytes isolated from the chimeric mice were demonstrated to be useful for evaluating the induction of CYP1A2 and 3A4;[25] in addition, CYP1A2 and 3A4 mRNA induction and expression from three different donor hepatocytes were reproduced in cryopreserved chimeric hepatocytes.[26] Due to the higher plating efficiency of fresh hepatocytes compared to cryopreserved cells, fresh chimeric hepatocytes would be useful for evaluating the human P450 induction abilities of xenobiotics.

We conclude that fresh and reproducible h-hepatocytes isolated from chimeric mice could be a useful tool in predicting the pharmacokinetics of chemical entities in addition to *in vivo* chimeric mouse studies. Comparative *in vitro* and *in vivo* studies using chimeric mice with the same donor could generate abundant data for resolving poorly understood phenomena and mechanisms.

Acknowledgments: We thank Mss. Y. Yoshizane, S. Nagai, and H. Kohno for providing excellent technical assistance.

References

1) Tateno, C., Yoshizane, Y., Saito, N., Kataoka, M., Utoh, R., Yamasaki, C., Tachibana, A., Soeno, Y., Asahina, K., Hino, H., Asahara, T., Yokoi, T., Furukawa, T. and Yoshizato, K.: Near completely humanized liver in mice shows human-type metabolic responses to drugs. *Am. J. Pathol.*, **165**: 901–912 (2004).
2) Katoh, M., Matsui, T., Nakajima, M., Tateno, C., Kataoka, M., Soeno, Y., Horie, T., Iwasaki, K., Yoshizato, K. and Yokoi, T.: Expression of human cytochrome P450 in chimeric mice with humanized liver. *Drug Metab. Dispos.*, **32**: 1402–1410 (2004).
3) Katoh, M., Matsui, T., Nakajima, M., Tateno, C., Soeno, Y., Horie, T., Iwasaki, K., Yoshizato, K. and Yokoi, T.: In vivo induction of human cytochrome P450 enzymes expressed in chimeric mice with humanized liver. *Drug Metab. Dispos.*, **33**: 754–763 (2005).
4) Katoh, M., Matsui, T., Okumura, H., Nakajima, M., Nishimura, M., Naito, S., Tateno, C., Yoshizato, K. and Yokoi, T.: Expression of human phase II enzymes in chimeric mice with humanized liver. *Drug Metab. Dispos.*, **33**: 1333–1340 (2005).
5) Wilkinson, G. R.: Drug metabolism and variability among patients in drug response. *N. Engl. J. Med.*, **352**: 2211–2221 (2005).
6) Populaire, P., Terlain, B., Pascal, S., Decouvelaere, B., Renard, A. and Thomas, J. P.: Biological behavior: serum levels, excretion and biotransformation of (3-benzoylphenyl)-2-propionic acid, or ketoprofen, in animals and men. *Ann. Pharm. Fr.*, **12**: 735–749 (1973).
7) Hashizume, K., Ohzone, Y., Adachi, Y., Ninomiya, A., Inoue, T. and Horie, T.: Characterization of chimeric mouse on in vivo metabolism of ketoprofen. *The Cell*, **40**: 26–29 (2008) in Japanese.
8) Ishizaki, T., Sasaki, T., Suganuma, T., Horai, Y., Chiba, K., Watanabe, M., Asuke, W. and Hoshi, H.: Pharmacokinetics of ketoprofen following single oral, intramuscular and rectal doses and after repeated oral administration. *Eur. J. Clin. Pharmacol.*, **18**: 407–414 (1980).
9) Ohashi, K., Tatsumi, K., Utoh, R., Takagi, S., Shima, M. and Okano, T.: Engineering liver tissues under the kidney capsule site provides therapeutic effects to hemophilia B mice. *Cell Transplant.*, in press
10) Sugihara, K., Kitamura, S., Yamada, T., Ohta, S., Yamashita, K., Yasuda, M. and Fujii-Kuriyama, Y.: Aryl hydrocarbon receptor (Ah)-mediated induction of xanthine oxidase/xanthine dehydrogenase activity by 2,3,7,8-tetrachlorodibenzo-p-dioxin. *Biochem. Biophys. Res. Commun.*, **281**: 1093–1099 (2001).
11) Nagano, M., Yamashita, S., Hirano, K., Ito, M., Maruyama, T., Ishihara, M., Sagehashi, Y., Oka, T., Kujiraoka, T., Hattori, H., Nakajima, N., Egashira, T., Kondo, M., Sakai, N. and Matsuzawa, Y.: Two novel missense mutations in the CETP gene in Japanese hyperalphalipoproteinemic subjects: high-throughput

assay by Invader assay. *J. Lipid Res.*, **43**: 1011–1018 (2002).
12) Kiyotani, K., Yamazaki, H., Fujieda, M., Iwano, S., Matsumura, K., Satarug, S., Ujjin, P., Shimada, T., Guengerich, F. P., Parkinson, A., Honda, G. Nakagawa, K., Ishizaki, T. and Kamataki, T.: Decreased coumarin 7-hydroxylase activities and CYP2A6 expression levels in humans caused by genetic polymorphism in CYP2A6 promoter region (CYP2A6*9). *Pharmacogenetics*, **13**: 689–695 (2003).
13) Katoh, M., Sawada, T., Soeno, Y., Nakajima, M., Tateno, C., Yoshizato, K. and Yokoi, T.: *In vivo* drug metabolism model for human cytochrome P450 enzyme using chimeric mice with humanized liver. *J. Pharm. Sci.*, **96**: 428–437 (2007).
14) Inoue, T., Nitta, K., Sugihara, K., Horie, T., Kitamura, S. and Ohta, S.: CYP2C9-catalyzed metabolism of S-warfarin to 7-hydroxywarfarin *in vivo* and *in vitro* in chimeric mice with humanized liver. *Drug Metab. Dispos.*, **36**: 2429–2433 (2008).
15) Rettie, A. E., Korzekwa, K. R., Kunze, K. L., Lawrence, R. F., Eddy, A. C., Aoyama, T., Gelboin, H. V., Gonzalez, F. J. and Trager, W. F.: Hydroxylation of warfarin by human cDNA-expressed cytochrome P-450: a role for P-4502C9 in the etiology of (S)-warfarin-drug interactions. *Chem. Res. Toxicol.*, **5**: 54–59 (1992).
16) Inoue, T., Sugihara, K., Ohshita, H., Horie, T., Kitamura, S. and Ohta, S.: Prediction of human disposition toward S-3H-warfarin using chimeric mice with humanized liver. *Drug Metab. Pharmacokinet.*, **24**: 153–160 (2009).
17) Steinberg, P., Fischer, T., Kiulies, S., Biefang, K., Platt, K. L., Oesch, F., Bottger, T., Bulitta, C., Kempf, P. and Hengstler, J.: Drug metabolizing capacity of cryopreserved human, rat, and mouse liver parenchymal cells in suspension. *Drug Metab. Dispos.*, **27**: 1415–1422 (1999).
18) Gebhardt, R., Hengstler, J. G., Muller, D., Glöckner, R., Buenning, P., Laube, B., Schmelzer, E., Ullrich, M., Utesch, D., Hewitt, N., Ringel, M., Hilz, B. R., Bader, A., Langsch, A., Koose, T., Burger, H. J., Maas, J. and Oesch, F.: New hepatocyte in vitro systems for drug metabolism: metabolic capacity and recommendations for application in basic research and drug development, standard operation procedures. *Drug Metab. Rev.*, **35**: 145–213 (2003).
19) Lau, Y. Y., Sapidou, E., Cui, X., White, R. E. and Cheng, K. C.: Development of a novel in vitro model to predict hepatic clearance using fresh, cryopreserved, and sandwich-cultured hepatocytes. *Drug Metab. Dispos.*, **30**: 1446–1454 (2002).
20) Hengstler, J. G., Utesch, D., Steinberg, P., Platt, K. L., Diener, B., Ringel, M., Swales, N., Fischer, T., Biefang, K., Gerl, M., Böttger, T. and Oesch, F.: Cryopreserved primary hepatocytes as a constantly available in vitro model for the evaluation of human and animal drug metabolism and enzyme induction. *Drug Metab. Rev.*, **32**: 81–118 (2000).
21) Diener, B., Utesch, D., Beer, N., Dürk, H. and Oesch, F.: A method for the cryopreservation of liver parenchymal cells for studies of xenobiotics. *Cryobiology*, **30**: 116–127 (1993).
22) Wang, Q., Jia, R., Ye, C., Garcia, M., Li, J. and Hidalgo, I. J.: Glucuronidation and sulfation of 7-hydroxycoumarin in liver matrices from human, dog, monkey, rat, and mouse. *In Vitro Cell Dev. Biol. Anim.*, **41**: 97–103 (2005).
23) Parkinson, A., Mudra, D. R., Johnson, C., Dwyer, A. and Carroll, K. M.: The effects of gender, age, ethnicity, and liver cirrhosis on cytochrome p450 enzyme activity in human liver microsomes and inducibility in cultured human hepatocytes. *Toxicol. Appl. Pharmacol.*, **199**: 193–209 (2004).
24) Kikuchi, R., McCown, M., Olson, P., Tateno, C., Morikawa, Y., Katoh, Y., Bourdet, D. L., Monshouwer, M. and Fretland, A. J.: Effect of hepatitis C virus infection on the mRNA expression of drug transporters and cytochrome p450 enzymes in chimeric mice with humanized liver. *Drug Metab. Dispos.*, **38**: 1954–1961 (2010).
25) Nishimura, M., Yokoi, T., Tateno, C., Kataoka, M., Takahashi, E., Horie, T., Yoshizato, K. and Naito, S.: Induction of human CYP1A2 and CYP3A4 in primary culture of hepatocytes from chimeric mice with humanized liver. *Drug Metab. Pharmacokinet.*, **20**: 121–126 (2005).
26) Yoshitsugu, H., Nishimura, M., Tateno, C., Kataoka, M., Takahashi, E., Soeno, Y., Yoshizato, K., Yokoi, T. and Naito, S.: Evaluation of human CYP1A2 and CYP3A4 mRNA expression in hepatocytes from chimeric mice with humanized liver. *Drug Metab. Pharmacokinet.*, **21**: 465–474 (2006).

HUMAN GENE THERAPY 21:40–50 (January 2010)

DOI: 10.1089/hum.2009.027

In Vivo Stable Transduction of Humanized Liver Tissue in Chimeric Mice via High-Capacity Adenovirus–Lentivirus Hybrid Vector

Shuji Kubo,[1,2] Miho Kataoka,[3] Chise Tateno,[3] Katsutoshi Yoshizato,[3,4] Yoshiko Kawasaki,[2] Takahiro Kimura,[1] Emmanuelle Faure-Kumar,[1] Donna J. Palmer,[5] Philip Ng,[5] Haruki Okamura,[2] and Noriyuki Kasahara[1]

Abstract

We developed hybrid vectors employing high-capacity adenovirus as a first-stage carrier encoding all the components required for *in situ* production of a second-stage lentivirus, thereby achieving stable transgene expression in secondary target cells. Such vectors have never previously been tested in normal tissues, because of the scarcity of suitable *in vivo* systems permissive for second-stage lentivirus assembly. Here we employed a novel murine model in which endogenous liver tissue is extensively reconstituted with engrafted human hepatocytes, and successfully achieved stable transduction by the second-stage lentivirus produced *in situ* from first-stage adenovirus. This represents the first demonstration of the functionality of adenoviral-lentiviral hybrid vectors in a normal parenchymal organ *in vivo*.

Introduction

ADENOVIRAL VECTORS (AdVs) have been successfully used *in vivo* to transduce various postmitotic tissues, but generally only transient gene expression can be achieved because of cytotoxic T-lymphocyte–mediated immune responses against viral genes retained in conventional AdVs, and their extremely low frequency of chromosomal integration (Harui *et al.*, 1999; Wivel *et al.*, 1999). More persistent expression can be maintained by high-capacity, helper-dependent AdVs (HDAdVs) from which all of the viral coding sequences have been removed (Parks *et al.*, 1996; Schiedner *et al.*, 1998; Kochanek, 1999; Kim *et al.*, 2001; Oka *et al.*, 2001), but its duration is still limited because of progressive dilution of the extrachromosomal HDAdV vector DNA as transduced cells divide. Treatment of hereditary diseases may require more stable, long-term transgene expression, which can be achieved only through permanent integration or ongoing episomal replication of vector DNA.

To overcome this limitation, various hybrid vector systems have been developed, which employ AdV as a first-stage delivery vehicle to efficiently enter target cells, but then utilize the machinery of integrating viruses or mobile genetic elements to achieve permanent chromosomal integration (Feng *et al.*, 1997; Caplen *et al.*, 1999; Lieber *et al.*, 1999; Recchia *et al.*, 1999; Tan *et al.*, 1999; Leblois *et al.*, 2000; Soifer *et al.*, 2001; Soifer *et al.*, 2002; Yant *et al.*, 2002; Kubo and Mitani, 2003; Dorigo *et al.*, 2004; Picard-Maureau *et al.*, 2004). Efficient two-stage transduction *in vitro* and stable long-term transgene expression have previously been demonstrated with AdV–transposon (Soifer *et al.*, 2001; Yant *et al.*, 2002), AdV–adeno-associated virus (Lieber *et al.*, 1999; Recchia *et al.*, 1999), AdV–retrovirus (Feng *et al.*, 1997; Caplen *et al.*, 1999; Soifer *et al.*, 2002), AdV–foamy virus (Picard-Maureau *et al.*, 2004), and AdV–lentivirus (Kubo and Mitani, 2003) vectors. In particular, Kubo and Mitani (2003) have demonstrated the ability of an AdV–lentivirus hybrid vector to efficiently enter a variety of cell types via the first-stage HDAdV and subsequently mediate *in situ* production of a human immunodeficiency virus (HIV)-derived second-stage lentiviral vector (LV), which then stably delivers a marker gene to neighboring cells. However, this hybrid vector generated second-stage LV pseudotyped with the vesicular stomatitis virus G glycoprotein (VSV-G), a highly fusogenic and toxic envelope

[1]Division of Digestive Diseases, Department of Medicine, University of California at Los Angeles, Los Angeles, CA 90095.
[2]Laboratory of Host Defenses, Institute for Advanced Medical Sciences, Hyogo College of Medicine, Nishinomiya, Hyogo 663-8501, Japan.
[3]Yoshizato Project, CLUSTER, Hiroshima Prefectural Institute of Industrial Science and Technology, Higashi-Hiroshima, Hiroshima 739-0046, Japan.
[4]Developmental Biology Laboratory and Hiroshima University 21st Century COE Program for Advanced Radiation Casualty Medicine, Department of Biological Science, Graduate School of Science, Higashi-Hiroshima, Hiroshima 739-8526, Japan.
[5]Center for Cell & Gene Therapy, Baylor College of Medicine, Houston, TX 77030.

protein (Ory *et al.*, 1996), which may result in unwanted cytotoxic effects in the primary target cells during LV production. Further, the ability of AdV-lentivirus hybrid vectors to stably transduce normal quiescent tissues *in vivo* has never previously been tested.

We have now developed an improved high-capacity AdV-lentivirus hybrid vector system, designated HL, and examined the ability of this new hybrid system to mediate efficient and stable gene transfer *in vitro* and *in vivo*. The first-stage HDAdV of the HL hybrid system directs the production of a minimal second-stage LV that retains less than 800 bp of HIV sequence (Chen *et al.*, 2002) and is pseudotyped with the murine leukemia virus (MLV) 4070A amphotropic envelope, which is much less cytotoxic than VSV-G. However, to test the transduction efficiency of the new HL hybrid vector system, target cells that can support *in situ* production of the HIV-derived second-stage LV are required. For *in vitro* experiments, human cell lines permissive for HIV replication can be employed. However, the requirement for human target cells presents a challenge to testing the functionality of the HL hybrid vector system *in vivo*, particularly with respect to its ability to stably transduce normal organs and tissues.

As nearly 90% of the input dose of AdV introduced *in vivo* accumulates in the liver upon intravenous injection (Kass-Eisler *et al.*, 1994; Huard *et al.*, 1995; Kubo *et al.*, 1997), and nearly 100% transduction of hepatocytes can be achieved at higher doses (Li *et al.*, 1993), the liver is an attractive target for *in vivo* testing of the HL system. However, multiple blocks to HIV replication have been reported in rodent cells, including cellular entry, reduced abundance of unspliced HIV-RNA and *gag* proteins, and defects in infectious particle assembly (Hofmann *et al.*, 1999; Bieniasz and Cullen, 2000; Mariani *et al.*, 2000). Therefore, to test the HL hybrid vector *in vivo*, we sought a humanized liver model that is permissive for HIV particle assembly.

Successful reconstitution of human liver tissue has recently been achieved in immunodeficient mice (Dandri *et al.*, 2001; Mercer *et al.*, 2001). Dandri *et al.* (2001) reported that cross-breeding of recombinant activation gene-2–deleted mice with transgenic mice expressing the hepatotoxic urokinase-type plasminogen activator (uPA) results in immunodeficient progeny which undergo progressive liver degeneration. These progeny were successfully transplanted with human hepatocytes, resulting in chimeric liver tissue with a replacement index of up to 15%, rendering these mice permissive for HBV infection (Dandri *et al.*, 2001). Similarly, Mercer *et al.* (2001) demonstrated that uPA/SCID mice bearing chimeric humanized livers with replacement index values of 50% could support HCV replication (Dandri *et al.*, 2001). More extensive repopulation has been difficult to achieve, likely because engrafted human hepatocytes produce complement factors, which appear to exert lethal effects in mice with higher replacement values. However, Tateno *et al.* (2004) and Yoshizato and colleagues (2004) have recently demonstrated that administration of a C5/C3 convertase inhibitor successfully rescued uPA/SCID mice whose chimeric livers proved to be almost completely repopulated with human hepatocytes exhibiting normal cytoarchitecture. The transduction efficiency of oncoretroviral vectors has previously been tested in this humanized liver model, and consistent with their inability to enter quiescent postmitotic cells, was found to be in the order of 5% (Emoto *et al.*, 2005). We have now utilized this unique chimeric liver model to test the ability of the HL hybrid system to mediate efficient entry by the first-stage HDAdV, *in situ* production of the second-stage LV, and stable transduction in fully humanized livers *in vivo*. To our knowledge, this represents the first report of *in vivo* testing of an AdV–lentivirus hybrid vector system in a normal parenchymal organ.

Materials and Methods

Cells

Cell lines including 293 (Graham *et al.*, 1977) (Microbix, Toronto, Canada), 293T (DuBridge *et al.*, 1987), and the Gli36 human glioma (Sena-Esteves *et al.*, 2000) were cultured in Dulbecco's modified Eagle's medium supplemented with 10% fetal calf serum (FCS; Omega, Tarzana, CA). Hep3B human hepatocellular carcinoma cells were cultured in Eagle's minimum essential medium supplemented with 10% FCS, 1 m*M* sodium pyruvate, and nonessential amino acids. Primary human hepatocytes and their specific medium were purchased from Cambrex (Baltimore, MD; CC-2591).

HL first-stage HDAdV construction and production

The phosphoglycerokinase promoter-driven green fluorescence protein (GFP) marker gene cassette, cytomegalovirus promoter (CMV)-driven *gag/pol/rev* lentiviral packaging cassette, simian virus 40 early promoter-driven MLV 4070A amphotropic envelope cassette, and minimal LV construct (Robbins *et al.*, 1998; Chen *et al.*, 2002) were sequentially cloned into the HDAdV plasmid pSTK120, which contains the human Ad5 inverted terminal repeat sequences and packaging signal, resulting in the construction of the complete HL vector plasmid, pHL. Additional details regarding the pHL construct, and the HIV-based minimal LV contained therein, are provided upon request.

The HL vector and control HDAdV cmv-GFP (Ad GFP) were prepared using the FLPe/*FRT* helper virus system (Umana *et al.*, 2001). The vectors were titrated on 293 cells for GFP expression, using a FACScalibur flow cytometer (Becton Dickinson, San Jose, CA), on day 2 post-infection, defined as transducing units per ml (TU/ml). Another control HDAdV, HDΔ28E4LacZ, was prepared as previously described (Palmer and Ng, 2003). Helper virus contamination levels were determined by Southern blot, as previously described (Kubo and Mitani, 2003).

Second-stage LV production after infection with HL first-stage HDAdV

To confirm production of LV in cells (Gli36, HeLa, Hep3B, HepG2 and human primary hepatocytes) infected by the HL vector, 4×10^5 cells of each were infected with various amounts of HL vector. The amount of vector used for each infection was based on the titer determined using each cell line. At 4 hr postinfection, the infected cells were washed three times with phosphate-buffered saline (PBS), and incubated in growth medium. At 48 hr postinfection, the virus-containing medium was harvested, centrifuged, filtered through a 0.45-μm pore filter, and used for titration on 293 cells by X-galactosidase (gal) staining to detect βgal expression. In preliminary experiments, the level of residual adenovirus carried over in the filtered supernatant medium after infection of primary cells at a multiplicity of infection (MOI) of 10, as

measured by flow cytometry for GFP expression in secondary cells, was less than 1%.

To inhibit lentiviral infection, 293 cells were infected with the viral supernatant in the presence or absence of 5 μM zidovudine (AZT; Sigma, St. Louis, MO).

To investigate the kinetics of LV vector production after HL vector infection, 4×10^5 Hep3B cells were infected with HL at various MOIs in six-well plates. The medium was collected at different time points and titrated on 293 cells, as described earlier.

Long-term culture experiments

Hep3B cells (2×10^5) were infected with the HL vector, at an MOI of 10, and incubated in the presence of AZT on a 10-cm dish. The cells were split at a ratio of 1:20 once a week, and expression of GFP was examined by flow cytometry. At each passage, DNA was extracted from a portion of the cells and analyzed for proviral integration by Southern hybridization. A part of the HL-infected cells were also plated on Lab-Tek chamber slides (Thermo Fisher Scientific, Rochester, NY). The next day, the cells were fixed for 10 min with 4% paraformaldehyde, washed with PBS, and incubated with 50 mM NH_4Cl in PBS for 5 min. The cells were permeabilized in 0.5% Triton/PBS for 5 min and then incubated for 30 min in 1% bovine serum albumin/PBS for blocking. The cells were incubated for 1 hr with a 1:1000 dilution of mouse anti-GFP monoclonal (Chemicon, Temecula, CA). Immunoreactivity for GFP was visualized with a 1:5000 dilution of goat anti-mouse immunoglobulin G (IgG) (H+L) Alexa Fluor 488. The cells were then incubated with a 1:1000 dilution of rabbit anti-βgal polyclonal (ab616; Abcam, Cambridge, MA). Immunoreactivities for βgal were visualized with a 1:5000 dilution of goat anti-rabbit IgG (H+L) Alexa Fluor 594 (Molecular Probes, Eugene, OR).

Animals

Chimeric mice with human liver were generated as previously described (Tateno *et al.*, 2004). Briefly, uPA/SCID mice were generated by crossing uPA mice [B6SJL-TgN(Alb1Plau)144Bri; The Jackson Laboratory, Bar Harbor, ME] with SCID mice (Fox Chase SCID C.B-17/Icr-*scid* Jcl; Clea Japan, Tokyo, Japan). The $uPA^{+/+}SCID^{+/+}$ mice were screened by polymerase chain reaction (PCR) and injected with $5.0–7.5\times10^5$ viable human hepatocytes (IVT079; In Vitro Technologies Inc., Baltimore, MD) through a small left-flank incision into the inferior splenic pole at 20–30 days after birth. The mice were injected intraperitoneally with 200 μl of 1.5 mg/ml Futhan (nafamostat mesilate, 6-amidino-2-naphthyl *p*-guanidinobenzoate dimethanesulfonate; gift from Torii Pharmaceutical, Tokyo, Japan) to enhance repopulation of the liver with human hepatocytes. The replacement index was estimated by serum level of human albumin as previously described (Tateno *et al.*, 2004). Generally, >5 mg/ml human albumin in the blood indicates high replacement index values of >70%, and mice screened in this manner were used for experiments at 6–8 weeks posttransplantation.

After injection with gadolinium (10 mg/kg body weight) to eliminate Kupffer cells (Lieber *et al.*, 1997), either HL vector (2×10^9 TU/200 ml) or buffer (PBS) was injected via tail vein, followed by sacrifice at 4 days or 4 weeks postinfection ($n=4$ per group). A portion of each liver sample was immediately digested into cell suspensions and used for flow cytometric analysis. The remaining portion was frozen in liquid nitrogen for isolation of genomic DNA or for frozen tissue sections. Immunofluorescence (IF) and immunohistochemistry (IHC) for GFP were performed on frozen liver sections using standard methods with GFP-specific antibodies (ab290; Abcam): goat anti-rabbit IgG-Alexa Fluor 488 for IF, or Vectastain ABC kit (Vector Laboratories, Burlingame, CA) and diaminobenzidine for IHC. IF for βgal was also performed using rabbit anti-βgal antibodies (ab616; Abcam) and goat anti-rabbit IgG-Alexa Fluor 594, as earlier. X-gal staining using standard methods was also performed on glutaraldehyde-fixed liver sections, and the proportion of βgal-positive cells was determined by image analysis using the SPOT digital imaging system and NIH ImageJ software (version 1.34). The replacement index of the mouse liver with human hepatocytes was also determined by IHC for human-specific cytokeratin-8 and -18 (CK8/18) as previously described (Tateno *et al.*, 2004) and is defined as the ratio of area occupied by human hepatocytes to the entire area examined. To assess any potential hepatotoxicity, sera were collected from mice at the time of scheduled sacrifice, that is, at 4 weeks after injection with HL vector or PBS, and serum levels of aspartate amino transferase (AST) were measured by automated colorimetric assay.

Molecular analysis of integrated LVs in the liver

High-molecular-weight genomic DNA was extracted from livers injected with HL vector or PBS. For detection of the stably integrated form of the second-stage LV after production from the first-stage HDAdV, high-molecular-weight genomic DNA (500 ng) was subjected to nested PCR to amplify lentiviral integration events close to or within *Alu* repeat sequences in the human genome (Nguyen *et al.*, 2002; Serafini *et al.*, 2004). Briefly, the first PCR (PCR1) was carried out using a sense oligomer specific for the conserved sequences of human *Alu* (*Alu*-s; 5′-TCCCAGCTACTCGGGAGGCTGAGG-3′) and an antisense oligomer specific for the PBS region of HIV-1 upstream of *gag* (5NC2-as; 5′-GAGTCCTGCGTCGAGAGAG-3′). All amplifications were done using 100 μl of reaction mixture containing 200 ng of genomic DNA, 0.4 mM of each dNTP, 0.8 μM of each sense and antisense primer, 5% dimethyl sulfoxide, and 2 U *Taq* DNA polymerase. After the first DNA denaturation at 95°C for 5 min, 30 amplification cycles were performed consisting of denaturation for 1 min at 94°C, annealing for 1 min at 60°C, and extension for 3 min at 72°C. One aliquot (1:100 dilution) of the first PCR products was subjected to a second PCR (PCR2) amplification using the nested primers, LTR9-s (5′-GCCTCAATAAAGCTTGCCTTG-3′) and U5PBS-as (spanning the U5LTR/PBS boundary region) (5′-GGCGCCACTGCTAGAGATTTT-3′), which amplified a fragment of 121 bp. The nested PCR conditions were similar to those of the first amplification, except for an annealing temperature of 55°C and an extension time of 1 min. Twenty amplification cycles were performed. In control reactions, genomic DNA that had not been subjected to the first round of PCR was also amplified using the second PCR primers to exclude the presence of residual nonintegrated vector DNA. As a loading control, the same DNA samples were subjected to a PCR that amplified a 610-bp region of human β-actin (5′-GATCATGTTTGAGACCTTCA-3′ and the reverse sequence 5′-ACC

TTGATCTTCATGGTGC-3'), with the following amplification conditions: 95°C for 2 min, then 30 cycles of 95°C for 30 sec, 65°C for 30 sec, and 72°C for 1 min, followed by a final extension at 72°C for 5 min. Amplification products were resolved on 1.5% agarose gel containing ethidium bromide and detected by ultraviolet transillumination.

The copy number of the integrated form of the lentiviral construct in each cell was determined by quantitative real-time PCR (Q-PCR) with βgal-specific primers and probe, designed using Primer Express software V. 1.0 (Applied Biosystems, Foster City, CA). Primer and probe sequences spanned a 91-bp region in the βgal-coding region, consisting of the following sequences: forward primer, 5'-CTATCCC GACCGCCTTACTG-3'; reverse primer, 5'-GTTTTCGCTCG GGAAGACGTA-3'; probe, 5'-FAM-CAGCGGTCAAAA CAG-TAMRA-3'. Amplification was performed in a reaction volume of 25 μl under the following conditions: 300 ng of high-molecular-weight genomic DNA, 1×Taqman universal PCR master mix (Applied Biosystems), 600 n*M* forward primer, 900 n*M* reverse primer, and 100 n*M* probe. Thermal cycling conditions were 2 min incubation at 50°C, 10 min at 95°C, followed by 40 cycles of successive incubation at 95°C for 15 sec and 60°C for 1 min. Standard curves were generated using serial dilutions of HL vector plasmid, pHL, from 5 to 50,000,000 copies in a background of 50,000 equivalents (300 ng) of untransduced genomic DNA from the chimeric mouse liver. Duplicate samples were amplified in an ABI Prism 7700 sequence detector with continuous fluorescence monitoring. Data were collected and analyzed using 7700 Sequence Detection System software v.1.6.3. (Applied Biosystems). The copy number per cell of integrated lentiviral construct was calculated as the average copy number divided by 50,000 cells (equivalent to 300 ng genomic DNA).

Statistical analysis

The results are presented as mean ± standard deviation. Statistical significance of differences was calculated using Student's *t*-test, and a *p*-value of <0.01 was considered significant.

Results

Design and production of the HL hybrid vector

The hybrid vector HL contains a complete set of HIV-derived lentiviral packaging components incorporated into an HDAdV (Fig. 1A), including (1) a multiple attenuated packaging construct expressing *gag-pol*, *rev*, and the *rev* response element sequence, (2) an envelope construct expressing amphotropic (i.e., broad mammalian host range) *env* from MLV strain 4070A, and (3) a minimal HIV-based LV transfer vector encoding a βgal marker gene driven by a methylation-resistant MLV promoter (MND promoter) (Chen *et al.*, 2002). As this transfer vector sequence contains a LV packaging signal so that its mRNA will be encapsidated by the coexpressed packaging and envelope components to form LV virions, the βgal transgene will not only be expressed in cells directly infected by the HDAdV, but also be transmitted to adjacent cells. The adenoviral backbone

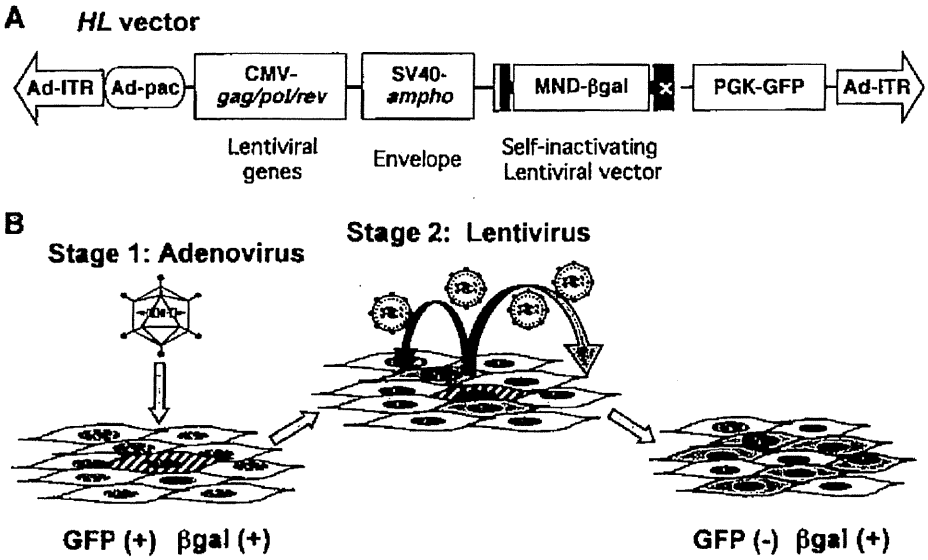

FIG. 1. Outline of the high-capacity adenovirus/lentivirus hybrid vector (HL vector) system. (A) Schematic structure of the HL vector. An HL vector is a helper-dependent adenoviral vector encoding expression cassettes for production of a lentiviral vector (LV) based on human immunodeficiency virus 1 (HIV-1). The HL vector has two inverted terminal repeats (Ad-ITR) and the packaging signal (Ad-pac) of human adenovirus type 5 and encodes four gene expression cassettes: (1) a self-inactivating minimal LV that contains the central polypurine tract, the woodchuck hepatitis virus posttranscriptional regulatory element, and the β-galactosidase gene (βgal) driven by the methylation-resistant murine leukemia virus LTR promoter (MND) (Robbins *et al.*, 1998; Chen *et al.*, 2002) as a marker; (2) HIV-*gag/pol/rev* coding sequences driven by cytomegalovirus (CMV) promoter; (3) the amphotropic murine leukemia virus envelope driven by the simian virus 40 early promoter (SV40) for pseudotyping of the lentivirus; and (4) the enhanced green fluorescent protein (GFP) driven by phosphoglycerokinase (PGK) promoter as a marker of the adenoviral backbone. (B) Two-stage transduction with the HL vector. The HL vector infects the initial target cells efficiently as an adenoviral vector and produces an LV *in situ*. The LV then infects surrounding secondary target cells and integrates into chromosomes for stable gene expression.

sequence also contains a GFP expression cassette unlinked to the LV components; the GFP marker gene will not be encapsidated into LV particles, thereby allowing specific quantitation of initial transduction by HDAdV itself. Thus, it is possible to distinguish between untransduced cells [GFP (−), βgal(−)], cells transduced by HL first-stage HDAdV only [GFP(+), βgal(+)], and cells transduced by HL second-stage LV [GFP(−), βgal(+)] (Fig. 1B).

The first-stage HDAdV was propagated using the FRT/FLPe helper system (Umana *et al.*, 2001). The GFP titers of purified HL vector preparations on 293 cells ranged from 4.1×10^9 to 1.8×10^{10} TU/ml. Vector stocks contained less than 0.1% helper virus contamination, as determined by Southern hybridization, using a probe for the adenoviral packaging signal (data not shown).

Infection with HL first-stage HDAdV results in production of functional second-stage LV

Following infection by the HL first-stage HDAdV vector at various MOIs, cell-free conditioned media from various human cell lines, including Gli36 (glioma), HeLa (cervical adenocarcinoma), and Hep3B and HepG2 (both hepatocellular carcinoma), were inoculated into fresh 293 cell cultures and tested for their ability to mediate secondary transmission of βgal expression. For all primary target cell lines tested, increasing MOI during first-stage HDAdV transduction correlated with increasing βgal transmission to secondary target cells (Fig. 2A). Further, βgal expression in secondary target cells was markedly suppressed by the reverse transcriptase inhibitor AZT, indicating that the observed transmission was indeed mediated by second-stage LV and was not due to carry-over of the first-stage HDAdV or pseudotransduction by overexpressed βgal protein (Fig. 2B). Of the cell lines tested, Gli36 and Hep3B produced the highest titers of LV (1.0×10^4 and 5.1×10^4 TU/ml, respectively, at MOI = 100) (Fig. 2A), which also correlated with high levels of p24 production (236 and 316 ng/ml, respectively). Primary human hepatocytes also produced LV at titers of 6.0×10^1, 1.0×10^3, and 1.2×10^4 TU/ml upon infection with 1, 10, and 100 μl of HL vector (4.0×10^8 TU/ml), respectively. Taken together, these findings indicate that the HL hybrid vector is

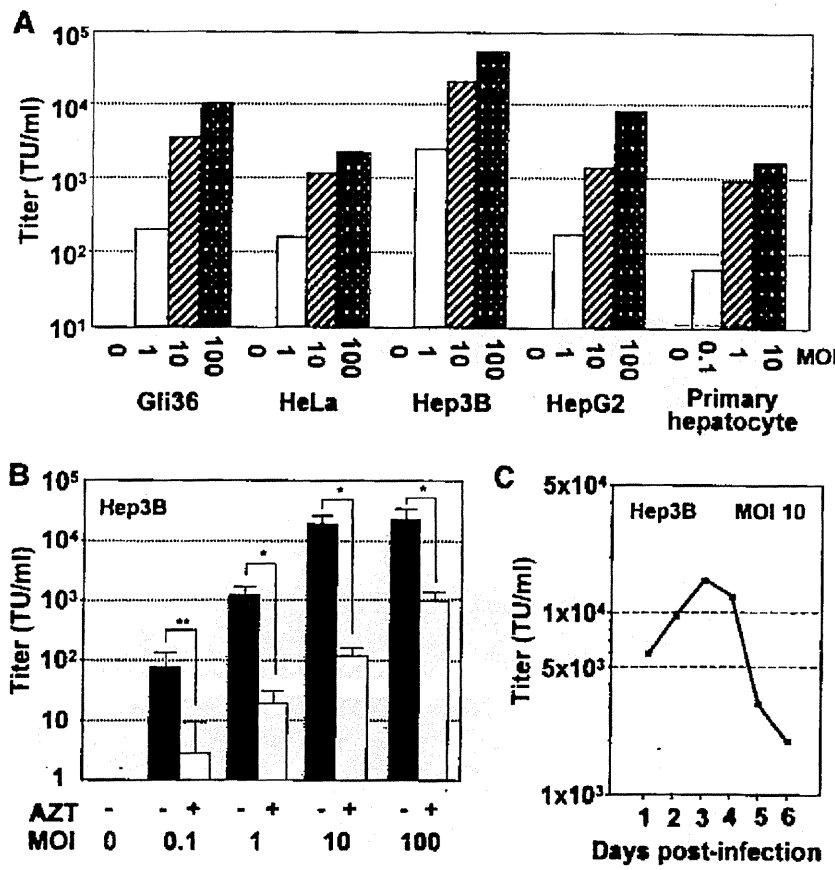

FIG. 2. Production of LV via HL vector system. (A) Production of LV in a variety of cell types after HL infection. Various cell lines indicated in the figure were infected with HL at multiplicity of infections (MOIs) of 1, 10, or 100. After 48 hr, viral supernatant was collected and titrated on 293 cells for βgal expression. (B) Production of LV following HL vector infection. Hep3B cells were infected with the HL vector at MOIs of 0.1, 1, 10, or 100. After 48 hr, viral supernatant was collected and titrated on 293 cells for βgal expression in the presence or absence of zidovudine (AZT, 5 μM). Data shown are average titers and standard deviations from the experiment performed in triplicate. Effect of AZT on titers was determined by Student's *t*-test (**$p < 0.05$, *$p < 0.01$). (C) Time course of lentiviral production from Hep3B cells infected with the HL vector. Hep3B cells were infected with HL at an MOI of 10 and monitored for up to 6 days. At different time points indicated in the figure, the medium was replaced, and the viral supernatant was titrated for βgal expression on 293 cells.

capable of directing the production of infectious LV particles from a variety of cell types, and that the LV yield is dependent upon the MOI and the target cell type.

To determine how long cells can produce LV after being infected with the HL first-stage HDAdV vector, a time-course experiment was performed. After infection of Hep3B cells with the HL first-stage HDAdV vector at an MOI of 10, the culture medium was harvested and replaced with fresh medium every day. The LV titers of the conditioned media harvested daily were measured on secondary target cells and were found to increase, reaching a peak level by day 3 post-HDAdV infection (1.3×10^4 TU/ml; Fig. 2C). Thereafter, HL-infected human cells continued to sustain LV production for several days (postinfection day 6 titer = 2.0×10^3 TU/ml).

In vitro persistence of second-stage LV-transduced cells following HL first-stage HDAdV infection

The spread of lentivirus in long-term cultures of HL-infected cells was examined by maintaining infected Hep3B in culture (Fig. 3A). As expected, GFP expression from the adenovirus backbone significantly decreased over time because of ongoing cell division-mediated dilution of HDAdV episomes in the culture. The percentage of GFP-positive cells

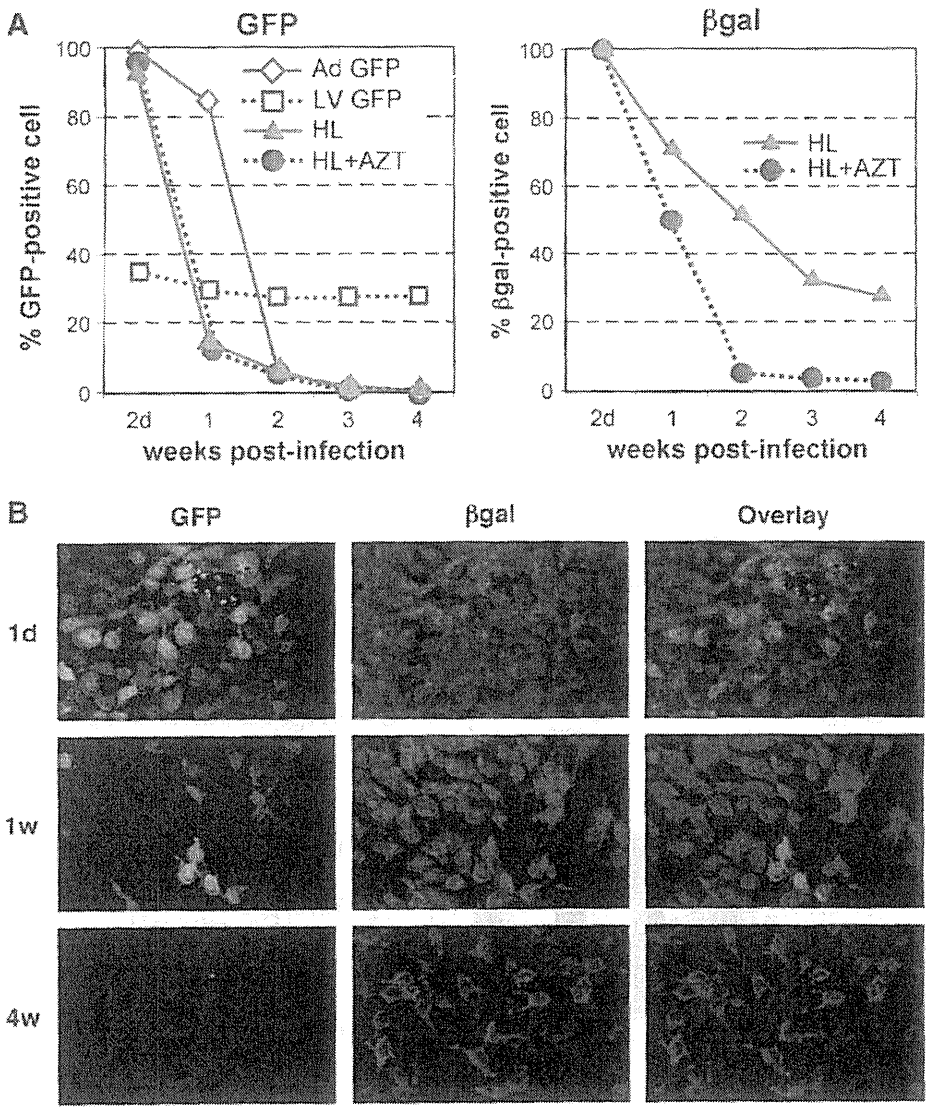

FIG. 3. Spread of LV-transduced cells and persistent gene expression following HL vector infection. (A) Transduction efficiencies of HL hybrid vector-infected cells. Hep3B cells (2×10^5) infected with the HL vector at an MOI of 10 were incubated overnight, and the cells were split the following day and cultivated in the presence (blue circle) or absence (red triangle) of AZT on a 10-cm dish. The control samples infected with an LV GFP (brown square) or an Ad GFP (green diamond) are also shown. The cells were passaged at a ratio of 1:20 every week, and expressions of GFP and βgal were examined. Data are representative of three independent experiments, all yielding similar results. (B) Persistent gene expression achieved via HL hybrid vector system in transformed human hepatocytes *in vitro*. Hep3B cells were infected with HL vector at an MOI of 10. The cells were passaged at a ratio of 1:20 every week. Expressions of GFP and βgal were analyzed by immunofluorescence staining using anti-GFP and anti-βgal antibody at the indicated time points after HL infection.

quickly decreased from > 90% to <2% within 2 weeks postinfection in the HL-infected cells (HL and HL + AZT) as well as in cells infected with control Ad GFP. Initially, a parallel decrease in βgal-positive cells was observed. However, 25% of the HL-infected cells (HL) remained βgal positive at 4 weeks postinfection, whereas those in the HL-infected/AZT-treated cells (HL + AZT) were <2% βgal positive within 2 weeks postinfection. Persistent βgal expression in the HL-infected cells (HL) was also confirmed by IF staining (Fig. 3B). Southern hybridization of high-molecular-weight genomic DNA extracted from the cells at week 4 confirmed LV proviral integration and a direct correlation between βgal expression and the copy number of the integrated βgal transgenes (data not shown). This also demonstrates that persistent βgal expression in the HL-infected cells is mediated by stable transduction with the HL second-stage LV vector.

In vivo *persistence of second-stage LV-transduced cells in humanized liver following intravenous administration of HL first-stage HDAdV*

In vivo testing of the HL vector system requires a model that is permissive for assembly of human lentivirus. We employed a unique humanized model in which endogenous murine hepatocytes are extensively replaced with human hepatocytes. The replacement indices, calculated as the frequency of human-specific CK8/18-positive regions relative to that of the entire examined area in the mouse liver (Tateno *et al.*, 2004), ranged from 63.7% to 86.6% (Fig. 4A). This model was found to be efficiently transduced by control HDAdV (HDΔ28E4LacZ) (Palmer and Ng, 2003) (data not shown), and so chimeric uPA/SCID mice with highly humanized livers were intravenously injected with the HL first-stage HDAdV vector.

First, GFP expression from the adenoviral backbone of the HL first-stage HDAdV in liver tissue was analyzed by flow cytometry. The results showed 7.64% ± 1.33% GFP-positive cells at 4 days postinfection and 0.21% ± 0.07% GFP-positive cells at 4 weeks postinfection. This reduction in GFP-positive hepatocytes was also confirmed by IF (Fig. 4B) and IHC (Fig. 4C).

On the other hand, βgal expression persisted for at least 4 weeks postinfection as shown by IF studies (Fig. 4D) and X-gal tissue staining (Fig. 4E). Quantitation by image analysis revealed that the percentage of βgal-positive cells increased from 16.21% ± 3.70% at 4 days, to 28.40 ± 4.92% at 4 weeks postinfection ($p = 0.0074$). The persistence of βgal expression suggested that stable integration by the second-stage LV might have occurred. To demonstrate integration of second-stage LV in human hepatocyte genomic DNA *in vivo*, nested *Alu*–lentivirus PCR was performed (Nguyen *et al.*, 2002; Serafini *et al.*, 2004). In this assay, the first round of PCR was performed using a sense primer specific for human *Alu* sequences and another primer specific for the lentiviral 5′ noncoding region as the antisense primer (*Alu*-s and 5NC2-as, respectively; Fig. 5A). As LV vectors randomly integrate at multiple sites and repetitive *Alu* sequences are scattered throughout the human genome, the first reaction generated products with variable sizes (Fig. 5B, PCR1). The second round of PCR, using nested primers within the viral LTR and the viral primer binding site, respectively ("LTR9-s" sense and "U5 PBS-as" antisense primers, as depicted in Fig. 5A), generated the expected 140-bp product from transduced liver tissues, but not from untransduced control liver (Fig. 5B, PCR1 + PCR2). Genomic DNA from transduced cells subjected only to second-round PCR amplification did not yield any signal, validating the inability of the nested primers alone to amplify any residual episomal LV sequences and confirming the requirement for first-round amplification with the *Alu*–lentivirus primers to detect integrated proviruses (Fig. 5B, PCR2). Although this is not a quantitative assay, taken together these results do demonstrate integration of the lentiviral sequences into the genome of human hepatocytes *in vivo*.

For further quantitative assessment of the percentage of cells expressing βgal from the lentivirus vector component, Q-PCR was again performed, this time using high-molecular-weight genomic DNA from each of liver tissues as the template and with primers and probe specific for the βgal gene. The Q-PCR results demonstrated that the percentage of βgal-positive cells was 13.8–56.6% at 4 weeks postinfection, correlating with the data obtained by Xgal staining (28.40% ± 4.92%) (Fig. 4E). These results indicate that *in situ* production and spread of second-stage LV had occurred in the humanized livers of chimeric mice following systemic administration of the HL first-stage HDAdV, and taken together with the above finding that the first-stage HDAdV was undetectable at 4 weeks postinfection, it is likely that βgal expression at a later time point is derived almost entirely from the second-stage LV.

To assess any potential vector-related hepatotoxicity, serum AST levels were measured and compared between HL vector-injected and control PBS-injected mice. It should be noted that the levels of serum liver enzymes in the uPA/SICD-based chimeric mouse model are generally high because of the ongoing hepatic expression of uPA, which mediates progressive destruction of murine hepatocytes and thereby allows gradual engraftment of human hepatocytes. Notably, however, there was no significant difference in the serum AST levels between HL-injected mice (272.5 ± 154.5 U/l) and PBS-treated group (453.0 ± 79.3 U/l) ($p = 0.1546$). Consistent with these findings, liver histology showed no significant difference between PBS- and HL vector-treated livers. Taken together with the serum AST levels, this indicates that the HL vector does not cause significant liver toxicity. In addition, as noted earlier, serum levels of human albumin remained at high values (>5 mg/ml) throughout these experiments, and replacement indices remained at high levels, ranging from 63.7% to 86.6% (Fig. 4A), further indicating that the HL vector does not show any selective toxicity that would alter the proportion of human hepatocytes.

Discussion

The liver has a variety of characteristics that make it a significant target for gene therapy (Ferry and Heard, 1998). As the liver is the site of essential metabolic pathways, it is involved in many inborn metabolic diseases. Moreover, because of its highly vascularized architecture and position as a portal to blood circulation, the liver can serve as a secretory organ for the systemic delivery of therapeutic proteins. Because of the fenestrated structure of its endothelium, the liver parenchyma is readily accessible to large molecules such as DNA or recombinant viruses via the blood stream. AdVs accumulate

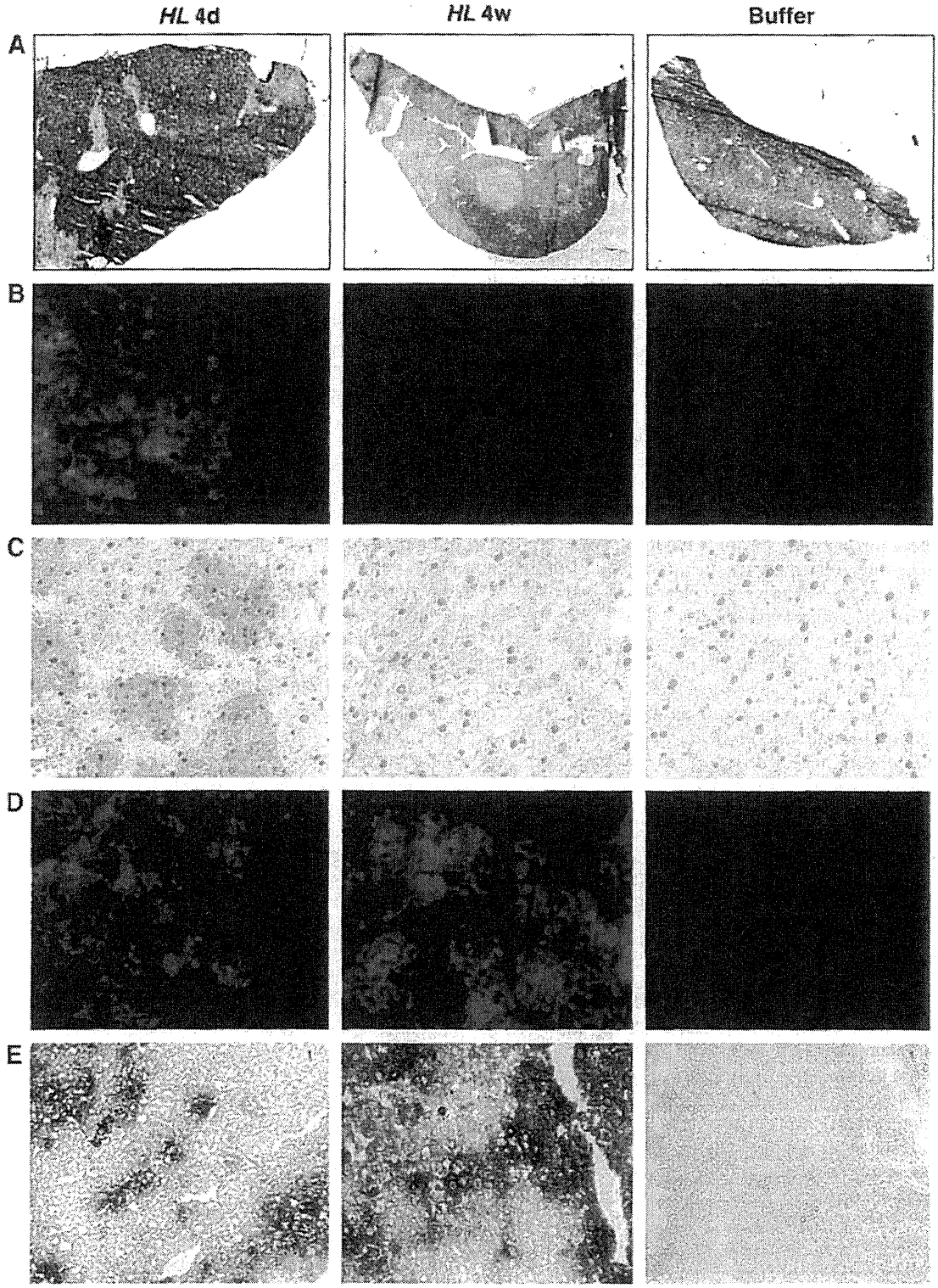

FIG. 4. *In vivo* transduction in humanized liver of the chimeric mice via HL hybrid vector system. The mice were injected with HL vector or phosphate-buffered saline (PBS) buffer. At indicated time points following HL infection, liver tissue was analyzed for GFP and βgal expression as follows: (**A**) Human CK8/18 immunostaining to determine replacement index of the mouse liver with human hepatocytes (human hepatocytes appear brown). Original magnification: 10×. (**B**) Immunofluorescence stain for GFP. Original magnification: 200×. (**C**) Immunohistochemical stain for GFP. Original magnification: 200×. (**D**) Immunofluorescence staining for βgal. Original magnification:×200. (**E**) X-gal staining. Original magnification:×100. Representative sections of each stain are shown.

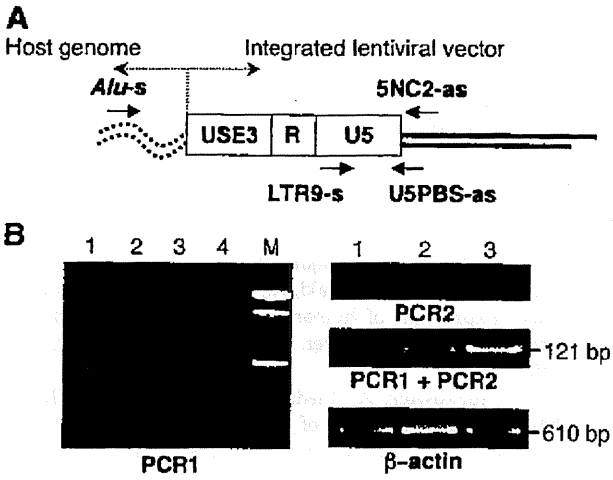

FIG. 5. Detection of integrated second-stage LV in liver tissue from chimeric mice after HL vector administration. (A) Design of nested polymerase chain reaction (PCR) analysis to amplify sequences spanning adjacent *Alu* repeats in the human genome (*Alu*-s and 5NC2-as) and the integrated lentiviral LTR (LTR9-s and U5PBS-as) (Nguyen *et al.*, 2002; Serafini *et al.*, 2004). (B) Result of nested PCR analysis: PCR1 and PCR2 correspond to the first and second rounds of nested PCR, respectively. M, 1-kb molecular mass size ladder (Invitrogen); lane 1, PBS-treated; lane 2, HL-infected, 4 days postinfection; lane 3, HL-infected, 4 weeks postinfection; lane 4, no DNA template. The 121-bp final amplification product is indicated. A 500-bp region of the human β-actin gene was amplified from the same samples as an internal control.

in the liver when injected intravenously (Kass-Eisler *et al.*, 1994; Huard *et al.*, 1995; Kubo *et al.*, 1997) and can achieve efficient hepatic gene delivery *in vivo* (Li *et al.*, 1993). The newer HDAdV system evades immune responses against transduced cells, thereby achieving long-term expression in the liver (Kim *et al.*, 2001; Oka *et al.*, 2001). However, HDAdV vectors still cannot overcome the limited duration of expression due to dilution of viral DNA as cells start to divide, a situation exacerbated if corrected hepatocytes have a selective growth advantage (Overturf *et al.*, 1996; De Vree *et al.*, 2000). Thus, the use of integrating vectors such as oncoretroviruses and lentiviruses has also been pursued.

However, hepatocytes are usually arrested in the G_0 phase of the cell cycle (Ferry and Heard, 1998), and the *in vivo* transduction efficiency of oncoretrovirus vectors is extremely low unless cell division is stimulated by growth factors or partial hepatectomy (Bosch *et al.*, 1996; Patijn *et al.*, 1998). In fact, the transduction efficiency of oncoretroviral vectors in the present uPA/SCID humanized liver model is only about 5% (Emoto *et al.*, 2005). Even though cellular mitosis is not absolutely required for lentiviral transduction, it has been reported that hepatocytes may be refractory even to lentiviral transduction unless they progress into the cell cycle (Park *et al.*, 2000), and certainly lentiviruses are incapable of efficiently transducing cells in G_0 phase, presumably because of lack of sufficient free nucleotide pools to support reverse transcription (Naldini *et al.*, 1996; Korin and Zack, 1998). As AdVs can readily infect nondividing cells (Benihoud *et al.*, 1999), it is quite advantageous to employ HDAdV as an efficient first-stage delivery vehicle for initial transient transduction of hepatocytes *in vivo*.

As the uPA/SCID chimeric mice are immunodeficient (Tateno *et al.*, 2004) and our hybrid vector is based on the HDAdV system which itself exhibits low immunogenicity (Kim *et al.*, 2001; Oka *et al.*, 2001), it might be anticipated that the HDAdV vector backbone would persist for an extended period of time in the engrafted human hepatocytes. Instead, expression of GFP in the humanized livers decreased significantly within 4 weeks after HL infection. It is possible that the toxic effects of HL-derived protein products (HIV-associated proteins and marker gene products) in the transduced cells might contribute to the activation of cell cycling in the liver; however, serum AST levels and liver histology of vector-injected animals were not significantly different from those of controls. In any case, loss of the HL-adenoviral episome would actually be advantageous to shutdown further production of the second-stage LV. To increase safety, a regulatable expression system could also be introduced into the hybrid vector to regulate LV production as reported previously (Kubo and Mitani, 2003).

Second-stage LV production *in situ* following HL vector-mediated hepatic gene transfer was assessed *in vivo* using chimeric mice in which the replacement indices indicated that the livers were almost completely repopulated with human hepatocytes. These chimeric mice have previously been shown to be a useful model for assessing the functions and pharmacological responses of human hepatocytes (Tateno *et al.*, 2004), but had never been previously employed in the evaluation of gene transfer efficiency with viral vectors.

In this humanized liver model, we observed persistent βgal expression associated with detection of integrated lentivirus sequences, despite a progressive decrease in GFP expression, suggesting that successful *in situ* production of LV had been achieved in HL-infected human hepatocytes. As noted earlier, stimulation of hepatocellular cycling after first-stage HDAdV infection might have accelerated the loss of adenoviral episomes, but may also have helped to enhance second-stage LV-mediated transduction of adjacent cells. As endogenous expression of the amphotropic envelope generally results in sequestration of the viral receptor and resistance to superinfection, it seems unlikely that cells initially transduced by the first-stage HDAdV would be reinfected with the second-stage LV. Genomic integration of the second-stage lentivirus vector was confirmed by PCR using human *Alu* and HIV LTR-specific primers. These data provide proof-of-principle for the use of the HL hybrid vector system to transduce liver parenchyma *in vivo* and for the use of the uPA/SCID mice as a model for gene delivery to human hepatocytes.

Acknowledgments

The authors thank Pedro Lowenstein for providing the FLP recombinase-based HDAdV helper system; Luigi Naldini and Didier Trono for the lentiviral packaging constructs; Stefan Kochanek for the STK plasmid; Paula Cannon for the minimal lentiviral vector; Chimoto Ohnishi for flow cytometric analysis; Maria Barcova, Celina Ngiam, and Ruth Margalit for their help during the preliminary phase of this work; and Karin Gaensler for helpful discussion. This work was supported by an NIH grant R01 CA93709 (to N.K.).

Disclosure Statement

No competing financial interests exist.

References

Benihoud, K., Yeh, P., and Perricaudet, M. (1999). Adenovirus vectors for gene delivery. Curr. Opin. Biotechnol. 10, 440–447.

Bieniasz, P.D., and Cullen, B.R. (2000). Multiple blocks to human immunodeficiency virus type 1 replication in rodent cells. J. Virol. 74, 9868–9877.

Bosch, A., McCray, P.B., Jr., Chang, S.M., Ulich, T.R., Simonet, W.S., Jolly, D.J., and Davidson, B.L. (1996). Proliferation induced by keratinocyte growth factor enhances *in vivo* retroviral-mediated gene transfer to mouse hepatocytes. J. Clin. Invest. 98, 2683–2687.

Caplen, N.J., Higginbotham, J.N., Scheel, J.R., Vahanian, N., Yoshida, Y., Hamada, H., Blaese, R.M., and Ramsey, W.J. (1999). Adeno-retroviral chimeric viruses as *in vivo* transducing agents. Gene Ther. 6, 454–459.

Chen, M., Kasahara, N., Keene, D.R., Chan, L., Hoeffler, W.K., Finlay, D., Barcova, M., Cannon, P.M., Mazurek, C., and Woodley, D.T. (2002). Restoration of type VII collagen expression and function in dystrophic epidermolysis bullosa. Nat. Genet. 32, 670–675.

Dandri, M., Burda, M.R., Torok, E., Pollok, J.M., Iwanska, A., Sommer, G., Rogiers, X., Rogler, C.E., Gupta, S., Will, H., Greten, H., and Petersen, J. (2001). Repopulation of mouse liver with human hepatocytes and *in vivo* infection with hepatitis B virus. Hepatology 33, 981–988.

De Vree, J.M., Ottenhoff, R., Bosma, P.J., Smith, A.J., Aten, J., and Oude Elferink, R.P. (2000). Correction of liver disease by hepatocyte transplantation in a mouse model of progressive familial intrahepatic cholestasis. Gastroenterology 119, 1720–1730.

Dorigo, O., Gil, J.S., Gallaher, S.D., Tan, B.T., Castro, M.G., Lowenstein, P.R., Calos, M.P., and Berk, A.J. (2004). Development of a novel helper-dependent adenovirus-Epstein-Barr virus hybrid system for the stable transformation of mammalian cells. J. Virol. 78, 6556–6566.

DuBridge, R.B., Tang, P., Hsia, H.C., Leong, P.M., Miller, J.H., and Calos, M.P. (1987). Analysis of mutation in human cells by using an Epstein-Barr virus shuttle system. Mol. Cell. Biol. 7, 379–387.

Emoto, C., Tateno, C., Hino, H., Amano, H., Imaoka, Y., Asahina, K., Asahara, T., and Yoshizato, K. (2005). Efficient *in vivo* xenogeneic retroviral vector-mediated gene transduction into human hepatocytes. Hum. Gene Ther. 16, 1168–1174.

Feng, M., Jackson, W.H., Jr., Goldman, C.K., Rancourt, C., Wang, M., Dusing, S.K., Siegal, G., and Curiel, D.T. (1997). Stable *in vivo* gene transduction via a novel adenoviral/retroviral chimeric vector [see comments]. Nat. Biotechnol. 15, 866–870.

Ferry, N., and Heard, J.M. (1998). Liver-directed gene transfer vectors. Hum. Gene Ther. 9, 1975–1981.

Graham, F.L., Smiley, J., Russell, W.C., and Nairn, R. (1977). Characteristics of a human cell line transformed by DNA from human adenovirus type 5. J. Gen. Virol. 36, 59–74.

Harui, A., Suzuki, S., Kochanek, S., and Mitani, K. (1999). Frequency and stability of chromosomal integration of adenovirus vectors. J. Virol. 73, 6141–6146.

Hofmann, W., Schubert, D., Labonte, J., Munson, L., Gibson, S., Scammell, J., Ferrigno, P., and Sodroski, J. (1999). Species-specific, postentry barriers to primate immunodeficiency virus infection. J. Virol. 73, 10020–10028.

Huard, J., Lochmuller, H., Acsadi, G., Jani, A., Massie, B., and Karpati, G. (1995). The route of administration is a major determinant of the transduction efficiency of rat tissues by adenoviral recombinants. Gene Ther. 2, 107–115.

Kass-Eisler, A., Falck-Pedersen, E., Elfenbein, D.H., Alvira, M., Buttrick, P.M., and Leinwand, L.A. (1994). The impact of developmental stage, route of administration and the immune system on adenovirus-mediated gene transfer. Gene Ther. 1, 395–402.

Katoh, M., Matsui, T., Nakajima, M., Tateno, C., Kataoka, M., Soeno, Y., Horie, T., Iwasaki, K., Yoshizato, K., and Yokoi, T. (2004). Expression of human cytochromes P450 in chimeric mice with humanized liver. Drug Metab. Dispos. 32, 1402–1410.

Kim, I.H., Jozkowicz, A., Piedra, P.A., Oka, K., and Chan, L. (2001). Lifetime correction of genetic deficiency in mice with a single injection of helper-dependent adenoviral vector. Proc. Natl. Acad. Sci. U.S.A. 98, 13282–13287.

Kochanek, S. (1999). High-capacity adenoviral vectors for gene transfer and somatic gene therapy. Hum. Gene Ther. 10, 2451–2459.

Korin, Y.D., and Zack, J.A. (1998). Progression to the G1b phase of the cell cycle is required for completion of human immunodeficiency virus type 1 reverse transcription in T cells. J. Virol. 72, 3161–3168.

Kubo, S., Kiwaki, K., Awata, H., Katoh, H., Kanegae, Y., Saito, I., Yamamoto, T., Miyazaki, J., Matsuda, I., and Endo, F. (1997). *In vivo* correction with recombinant adenovirus of 4-hydroxyphenylpyruvic acid dioxygenase deficiencies in strain III mice. Hum. Gene Ther. 8, 65–71.

Kubo, S., and Mitani, K. (2003). A new hybrid system capable of efficient lentiviral vector production and stable gene transfer mediated by a single helper-dependent adenoviral vector. J. Virol. 77, 2964–2971.

Leblois, H., Roche, C., Di Falco, N., Orsini, C., Yeh, P., and Perricaudet, M. (2000). Stable transduction of actively dividing cells via a novel adenoviral/episomal vector. Mol. Ther. 1, 314–322.

Li, Q., Kay, M.A., Finegold, M., Stratford-Perricaudet, L.D., and Woo, S.L. (1993). Assessment of recombinant adenoviral vectors for hepatic gene therapy. Hum. Gene Ther. 4, 403–409.

Lieber, A., He, C.Y., Meuse, L., Schowalter, D., Kirillova, I., Winther, B., and Kay, M.A. (1997). The role of Kupffer cell activation and viral gene expression in early liver toxicity after infusion of recombinant adenovirus vectors. J. Virol. 71, 8798–8807.

Lieber, A., Steinwaerder, D.S., Carlson, C.A., and Kay, M.A. (1999). Integrating adenovirus-adeno-associated virus hybrid vectors devoid of all viral genes. J. Virol. 73, 9314–9324.

Mariani, R., Rutter, G., Harris, M.E., Hope, T.J., Krausslich, H.G., and Landau, N.R. (2000). A block to human immunodeficiency virus type 1 assembly in murine cells. J. Virol. 74, 3859–3870.

Mercer, D.F., Schiller, D.E., Elliott, J.F., Douglas, D.N., Hao, C., Rinfret, A., Addison, W.R., Fischer, K.P., Churchill, T.A., Lakey, J.R., Tyrrell, D.L., and Kneteman, N.M. (2001). Hepatitis C virus replication in mice with chimeric human livers. Nat. Med. 7, 927–933.

Naldini, L., Blomer, U., Gallay, P., Ory, D., Mulligan, R., Gage, F.H., Verma, I.M., and Trono, D. (1996). *In vivo* gene delivery and stable transduction of nondividing cells by a lentiviral vector. Science 272, 263–267.

Nguyen, T.H., Oberholzer, J., Birraux, J., Majno, P., Morel, P., and Trono, D. (2002). Highly efficient lentiviral vector-mediated

transduction of nondividing, fully reimplantable primary hepatocytes. Mol. Ther. 6, 199–209.

Oka, K., Pastore, L., Kim, I.H., Merched, A., Nomura, S., Lee, H.J., Merched-Sauvage, M., Arden-Riley, C., Lee, B., Finegold, M., Beaudet, A., and Chan, L. (2001). Long-term stable correction of low-density lipoprotein receptor-deficient mice with a helper-dependent adenoviral vector expressing the very low-density lipoprotein receptor. Circulation 103, 1274–1281.

Ory, D.S., Neugeboren, B.A., and Mulligan, R.C. (1996). A stable human-derived packaging cell line for production of high titer retrovirus/vesicular stomatitis virus G pseudotypes. Proc. Natl. Acad. Sci. U.S.A. 93, 11400–11406.

Overturf, K., Al-Dhalimy, M., Tanguay, R., Brantly, M., Ou, C.N., Finegold, M., and Grompe, M. (1996). Hepatocytes corrected by gene therapy are selected *in vivo* in a murine model of hereditary tyrosinaemia type I. Nat. Genet. 12, 266–273.

Palmer, D., and Ng, P. (2003). Improved system for helper-dependent adenoviral vector production. Mol. Ther. 8, 846–852.

Park, F., Ohashi, K., Chiu, W., Naldini, L., and Kay, M.A. (2000). Efficient lentiviral transduction of liver requires cell cycling *in vivo*. Nat. Genet. 24, 49–52.

Parks, R.J., Chen, L., Anton, M., Sankar, U., Rudnicki, M.A., and Graham, F.L. (1996). A helper-dependent adenovirus vector system: Removal of helper virus by Cre-mediated excision of the viral packaging signal. Proc. Natl. Acad. Sci. U.S.A. 93, 13565–13570.

Patijn, G.A., Lieber, A., Schowalter, D.B., Schwall, R., and Kay, M.A. (1998). Hepatocyte growth factor induces hepatocyte proliferation *in vivo* and allows for efficient retroviral-mediated gene transfer in mice. Hepatology 28, 707–716.

Picard-Maureau, M., Kreppel, F., Lindemann, D., Juretzek, T., Herchenroder, O., Rethwilm, A., Kochanek, S., and Heinkelein, M. (2004). Foamy virus—adenovirus hybrid vectors. Gene Ther. 11, 722–728.

Recchia, A., Parks, R.J., Lamartina, S., Toniatti, C., Pieroni, L., Palombo, F., Ciliberto, G., Graham, F.L., Cortese, R., La Monica, N., and Colloca, S. (1999). Site-specific integration mediated by a hybrid adenovirus/adeno-associated virus vector. Proc. Natl. Acad. Sci. U.S.A. 96, 2615–2620.

Robbins, P.B., Skelton, D.C., Yu, X.J., Halene, S., Leonard, E.H., and Kohn, D.B. (1998). Consistent, persistent expression from modified retroviral vectors in murine hematopoietic stem cells. Proc. Natl. Acad. Sci. U.S.A. 95, 10182–10187.

Schiedner, G., Morral, N., Parks, R.J., Wu, Y., Koopmans, S.C., Langston, C., Graham, F.L., Beaudet, A.L., and Kochanek, S. (1998). Genomic DNA transfer with a high-capacity adenovirus vector results in improved *in vivo* gene expression and decreased toxicity. Nat. Genet. 18, 180–183.

Sena-Esteves, M., Saeki, Y., Fraefel, C., and Breakefield, X.O. (2000). HSV-1 amplicon vectors—simplicity and versatility. Mol. Ther. 2, 9–15.

Serafini, M., Naldini, L., and Introna, M. (2004). Molecular evidence of inefficient transduction of proliferating human B lymphocytes by VSV-pseudotyped HIV-1-derived lentivectors. Virology 325, 413–424.

Soifer, H., Higo, C., Kazazian, H.H., Jr., Moran, J.V., Mitani, K., and Kasahara, N. (2001). Stable integration of transgenes delivered by a retrotransposon-adenovirus hybrid vector. Hum. Gene Ther. 12, 1417–1428.

Soifer, H., Higo, C., Logg, C.R., Jih, L.J., Shichinohe, T., Harboe-Schmidt, E., Mitani, K., and Kasahara, N. (2002). A novel, helper-dependent, adenovirus-retrovirus hybrid vector: Stable transduction by a two-stage mechanism. Mol. Ther. 5, 599–608.

Tan, B.T., Wu, L., and Berk, A.J. (1999). An adenovirus-Epstein-Barr virus hybrid vector that stably transforms cultured cells with high efficiency. J. Virol. 73, 7582–7589.

Tateno, C., Yoshizane, Y., Saito, N., Kataoka, M., Utoh, R., Yamasaki, C., Tachibana, A., Soeno, Y., Asahina, K., Hino, H., Asahara, T., Yokoi, T., Furukawa, T., and Yoshizato, K. (2004). Near completely humanized liver in mice shows human-type metabolic responses to drugs. Am. J. Pathol. 165, 901–912.

Umana, P., Gerdes, C.A., Stone, D., Davis, J.R., Ward, D., Castro, M.G., and Lowenstein, P.R. (2001). Efficient FLPe recombinase enables scalable production of helper-dependent adenoviral vectors with negligible helper-virus contamination. Nat. Biotechnol. 19, 582–585.

Wivel, N.A., Gao, G.-P., and Wilson, J.M. (1999). Adenovirus vectors. In *The Development of Human Gene Therapy*. T. Friedmann, ed. (Cold Spring Harbor Laboratory Press, Cold Spring Harbor, NY) pp. 87–110.

Yant, S.R., Ehrhardt, A., Mikkelsen, J.G., Meuse, L., Pham, T., and Kay, M.A. (2002). Transposition from a gutless adeno-transposon vector stabilizes transgene expression *in vivo*. Nat. Biotechnol. 20, 999–1005.

Address correspondence to:
Dr. Shuji Kubo
Laboratory of Host Defenses
Institute for Advanced Medical Sciences
Hyogo College of Medicine
1-1, Mukogawa-cho, Nishinomiya
Hyogo 663-8501
Japan

E-mail: s-kubo@hyo-med.ac.jp

Received for publication February 22, 2009;
accepted after revision September 2, 2009.

Published online: December 17, 2009.

Hindawi Publishing Corporation
PPAR Research
Volume 2009, Article ID 476217, 11 pages
doi:10.1155/2009/476217

Review Article

A Human Hepatocyte-Bearing Mouse: An Animal Model to Predict Drug Metabolism and Effectiveness in Humans

Katsutoshi Yoshizato[1,2] and Chise Tateno[1]

[1] *PhoenixBio, Kagamiyama, 3-4-1 Kagamiya, Higashihiroshima 739-0046, Japan*
[2] *Osaka City University Gradate School of Medicine, 1-4-3 Asahi-machi, Abeno-ku, Osaka 545-8585, Japan*

Correspondence should be addressed to Katsutoshi Yoshizato, katsutoshi.yoshizato@phoenixbio.co.jp

Received 9 April 2009; Accepted 13 July 2009

Recommended by James P. Hardwick

Preclinical studies to predict the efficacy and safety of drugs have conventionally been conducted almost exclusively in mice and rats as rodents, despite the differences in drug metabolism between humans and rodents. Furthermore, human (*h*) viruses such as hepatitis viruses do not infect the rodent liver. A mouse bearing a liver in which the hepatocytes have been largely repopulated with *h*-hepatocytes would overcome some of these disadvantages. We have established a practical, efficient, and large-scale production system for such mice. Accumulated evidence has demonstrated that these hepatocyte-humanized mice are a useful and reliable animal model, exhibiting *h*-type responses in a series of in vivo drug processing (adsorption, distribution, metabolism, excretion) experiments and in the infection and propagation of hepatic viruses. In this review, we present the current status of studies on chimeric mice and describe their usefulness in the study of peroxisome proliferator-activated receptors.

1. Introduction

The human (*h*)-body consists of approximately 30 organs, each of which fulfills a specific function, autonomously yet cooperatively with other organs, to maintain life. The liver is essential to (*h*)-life, as it participates in the control of energy balance and plays central roles in the metabolism and excretion of ingested food and chemicals. Knowledge of the mechanisms underlying the functions of the *h*-liver is important for understanding the biology of the liver as well as for clinically treating liver-damaged patients and for studying drug pharmacology in humans. The ideal approach to elucidating the mechanisms responsible for liver functions would be to perform experiments using the *h*-liver *in situ*, but of course this approach is not realistic. Therefore, scientists have taken two other approaches: in vitro examination of samples isolated from the *h*-body (in vitro/human), and in vivo examinations using animals (in vivo/animal). Although these two approaches, separately and together, have revealed much about the mechanisms governing the functions and morphology of the *h*-liver, they are inherently limited by the complexity of the biological phenomena and the species differences in homologous mechanisms between animals and humans.

The complexity of a biological phenomenon results from the required mutual interactions of multiple different components. The specific cells that represent an organ's functions are collectively termed parenchymal cells. For example, the parenchymal cells of the liver are hepatocyte, because they perform liver-specific functions such as the synthesis and secretion of serum proteins and the synthesis of metabolism-related enzymes, including liver-specific cytochrome P450 (CYP450) proteins. However, hepatocytes by themselves are unable to fulfill liver functions and require the cooperation of nonparenchymal liver cells such as hepatic blood vessels, bile duct biliary cells, Kupffer cells, and stellate cells in the space of Disse, located between the hepatic plate and the sinusoids [1]. The portal vein is the major import route for nutrients to the liver, via the hepatic sinusoids, from the small and most of the large intestine, the spleen, and the pancreas. Nutrients and oxygen in the sinusoids and secretory proteins in the hepatocytes are exchanged through the space of Disse. Stellate cells, the major cell type producing extracellular matrix components in the liver, are located

adjacent to the hepatocytes and the sinusoidal endothelial cells [2]. Hepatocytes, endothelial cells, and stellate cells represent 65, 21, and 6%, respectively, of the *h*-liver and are the main cells responsible for liver functions [1].

Interactive cooperation among different cells types is a principal way in which a multicellular entity is able to function as a living system. It is also a major source of the limitations in in vitro/human studies. To date, no studies have successfully reconstituted an in vitro/*h*-liver system that perfectly mimics the events that occur in the *h*-liver in vivo. This limitation has prompted a search for an in vivo/animal experimental system appropriate for providing animal data that can be extrapolated to humans. However, animal models must address the challenge of species differences in the genes and proteins associated with a biological phenomenon.

The liver processes nutrients from the gut and intestines into proteins, lipids, and carbohydrates. It also serves an endocrine function by secreting albumin (Alb), most coagulation factors, several plasma carrier proteins, and lipids into the blood. In addition, the liver synthesizes bile and secretes it into the digestive tract. The elaborate histological structure of the liver optimizes these functions [3]. Hepatocytes are well organized in an aggregated association (the hepatic epithelium) of polarized hepatocytes, creating small apical domains that line the channels between cells (canaliculi). These channels connect to the bile ducts, which drain into the intestine. The basal sides of the hepatocytes are juxtaposed to the fenestrated endothelium of the sinusoids, into which blood flows from the arterial and intestinal portal circulations before emptying into the venous circulation [4].

h-Hepatocytes are indispensable for an in vitro/human liver study. Nevertheless, the preparation of *h*-hepatocytes in sufficient numbers for experimental purposes is difficult because the source is very limited and because *h*-hepatocytes do not abundantly proliferate and grow in vitro. This led us to create a mouse (*m*) bearing a liver composed almost entirely of *h*-hepatocytes. This approach may simultaneously abolish the limitations of both in vitro/human and in vivo/animal studies. With this *m*-model, a small number of available *h*-hepatocytes could abundantly proliferate in the *m*-liver for use in in vitro/human studies. Furthermore, these mice would provide a superior new type of model animal for in vivo/animal studies, because fewer species differences would exist with respect to liver functions.

We have called this type of mouse a "liver-humanized mouse," or simply a chimeric mouse, although the correct name should be "hepatocyte-humanized mouse." The idea of a *h*-liver chimeric mouse was originally described by Brinster's group in 1995 [5] and was actualized by the two groups in 2001 to study *h*-hepatitis B virus (*h*-HBVs) [6] and *h*-HCV infections [7], and later, in 2004, by us to study the in vivo growth capacity of *h*-hepatocytes and the gene and protein expression of CYPs [8]. One year later, a detailed morphological study of a chimeric *m*-liver was reported by Meuleman et al. [9]. Kneteman and Mercer briefly reviewed the current chimeric mouse studies [10]. In this article, we review the studies on chimeric mice, including their short historical background, usefulness in testing *h*-type metabolism of clinically usable drugs, and potential use in examining *h*-type peroxisome proliferator-activated receptors (PPARs), especially PPARα, which plays key roles in the metabolism of xenobiotics in an animal species-dependent manner. We demonstrate that *h*-hepatocytes propagated in a chimeric *m*-liver and then isolated can serve as normal *h*-hepatocytes for an in vitro/human model [11].

2. A Mouse Bearing Transplanted Homogenic and Xenogenic Hepatocytes

To study neonatal bleeding disorders, transgenic mice ($Tg_{Alb\text{-}uPA}$) carrying a tandem array of about four Albumin promoter/enhancer-driven urokinase-type plasminogen activator (uPA) genes were created [12]. Their hepatocytes over-produce murine urokinase, and the liver becomes severely hypofibrinogenemic, which accelerates hepatocyte death. Sandgren et al. [13] developed a model of liver regeneration in $Tg_{Alb\text{-}uPA}$ mice, in which a chronic stimulus for liver growth was generated due to a functional liver deficit. When a hepatocyte stochastically deleted the deleterious transgene, the hepatocytes of mice hemizygous for the transgene started to replicate and selectively expanded to regain the original size of the liver. Transgene expression in the replicating hepatocytes was abolished because of a DNA rearrangement that affected the transgene tandem array. This permitted the individuals to survive beyond birth, and the plasma uPA concentrations gradually returned to normal by 2 months of age. The transgene-deficient cells formed clonal colonies called hepatic nodules. These nodules expanded and replaced the surrounding transgene-active cells, which could not replicate because of cellular damage. Eventually, the transgene-deficient cells replaced the entire liver. This study demonstrates the usefulness of the $Tg_{Alb\text{-}uPA}$ mouse for examining the replicative capacity of not only *m*-hepatocytes, which was successfully done by transplanting hepatocytes isolated from adult mice into the transgenic mice [14], but also hepatocytes of mammals that acquire immunotolerance as follows.

Rhim et al. [5] introduced the Alb-uPA transgene into immunotolerant nu/nu mice by mating $Tg_{Alb\text{-}uPA}$ mice with Swiss athymic nude mice, generating immunotolerant $Tg_{Alb\text{-}uPA}$ mice ($Tg_{Alb\text{-}uPA}$/NUDE mice). Rat (*r*) liver cells were transplanted into the livers of $Tg_{Alb\text{-}uPA}^{+/+}$/NUDE mice homozygous for the transgene. The host livers that had not been transplanted with *r*-liver cells were completely pale (white). In contrast, those with *r*-liver cells had white regions, representing the area composed only of transgene-expressing host *m*-cells, and red regions, representing the area composed of transgene-deleted host *m*-cells, repopulated *r*-cells, or both. Immunohistochemical analysis with antibodies against *r*-hepatocytes confirmed that the red region was composed primarily of *r*-hepatocytes. The completely regenerated transgenic *m*-livers resemble normal *m*-livers in color, shape, and size. Southern blot analysis demonstrated that up to 56% of the DNA was of rat origin, which agreed well with the parenchymal cell occupancy rate in the liver. These findings strongly support the idea that the host liver was chimeric, with *r*-parenchyma and *m*-nonparenchymal cells,

which included vessels, bile ducts, and associated connective tissues. The ratio of the liver weight to the body weight was 6.8%, which was similar to that of the non-transgenic control mice (5.8%), indicating that the rat-mouse (*r/m*) chimeric livers were able to normally terminate growth. The successful generation of a healthy mouse with a chimeric liver indicates that *r*-parenchymal and *m*-nonparenchymal cells were able to communicate with each other to reconstitute a functional liver, despite the species difference.

Hepatocytes initiate and terminate proliferation under the influence of nonparenchymal cells [1]. Thus, the normal progression and termination of *r/m*-chimeric liver regeneration implies that *r*-hepatocytes produce surface proteins that interact correctly with soluble *m*-factors, *m*-extracellular matrix, and *m*-surface proteins on *m*-nonparenchymal cells. The successful replacement of $Tg_{Alb\text{-}uPA}^{+/+}$/NUDE*m*-livers with *r*-hepatocytes raised the exciting possibility that *m*-livers could also be reconstituted with *h*-hepatocytes [5].

3. Repopulation of *h*-Hepatocytes in *m*-Liver

In two previous studies to generate a mouse with a *h*-hepatocyte-mouse (*h/m*) chimeric liver, Rug-2-knockout mice [6] and severe combined immunodeficient (SCID) mice [7] were used as immunodeficient mating partners for uPA transgenic mice. We mated SCID mice ($mice_{SCID}$) with $Tg_{Alb\text{-}uPA}^{+/+}$ mice to yield liver-injured SCID mice ($mice_{Alb\text{-}uPA/SCID}$) [8]. Normal *h*-hepatocytes, $\sim 10^6$ viable cells per mouse, were transplanted into the livers of these mice at 20–30 days after birth. The *h*-hepatocytes engrafted the liver at rates as high as 96% and progressively repopulated it. The repopulation after *h*-hepatocyte transplantation was easily monitored by the increase in the *h*-Alb concentration in the host blood, and the expansion of *h*-hepatocyte colonies was visualized by immunohistological staining of liver sections with *h*-specific anti-cytokeratin (CK) 8/18 antibodies. The ratio of the number of engrafted *h*-hepatocytes to total hepatocytes (*m*- and *h*-hepatocytes) in the host liver, which is the replacement index (RI), was determined by calculating the ratio of the area occupied by hCK8/18-positive hepatocytes to the entire area examined in immunohistochemical sections of seven lobes. It was demonstrated that sustained engraftment of *h*-hepatocytes occurs in homozygous Alb-uPA transgenic ($Tg_{Alb\text{-}uPA}^{+/+}$) mice, but not in hemizygous transgenic ($Tg_{Alb\text{-}uPA}^{+/-}$) mice. The *h*-hepatocytes started to proliferate around 7 days after transplantation. Their colonies gradually became larger and were almost confluent at around 70 days, when the RI was as high as 96%. Immunohistological staining of liver sections for type IV collagen, laminin, stabilin (a liver endothelial cell marker), BM8 (a Kupffer cell marker), and desmin (a hepatic stellate cell marker) demonstrated the chimeric nature of the liver (Figure 1). The interactions between hepatocytes and stellate cells are critical for physiological and pathological conditions of the liver [15]. Close and seemingly normal associations of *h*-hepatocytes with *m*-stellate cells were immunohistologically visualized by staining with specific antibodies against *h*-CK8/18 (*h*-hepatocytes) and *m*-desmin (*m*-stellate cells) (Figure 2). These results clearly show that the chimeric *m*-livers with a high RI consisted of parenchymal cells (mostly *h*-cells with a low percentage of *m*-cells), *m*-nonparenchymal cells, and *m*-ECMs, in agreement with a previous study [9]. There was good correlation between the RI and the mRNA expression levels of housekeeping genes such as *h*-Alb and *h*-transferrin, supporting the notion that transplanted *h*-hepatocytes are functional [16]. In our experience, mice with >6 mg/mL *h*-Alb in the blood had an RI >70%. Our histological studies illustrated that the *h*-hepatocytes were well organized and surrounded by *m*-nonparenchymal cells, and they reconstituted the normal tissues specific to a normal functional liver (described in Section 1), despite the large species difference between humans and mice.

We chose robustly growing young mice as hosts. These mice were able to not only survive but also grow, although relatively slowly, and increase their body weight by >50% of their original weight, during the replacement of host *m*-hepatocytes with *h*-counterparts. These simple animal experiments made us realize that *m*-cells and *h*-hepatocytes were able to mutually communicate to maintain life: *m*-cells supported the proliferation of *h*-hepatocytes, and *h*-hepatocytes supported the growth of the young mouse. The host liver of a $mouse_{Alb\text{-}uPA/SCID}$ is congenitally damaged owing to uPA overproduction, low blood levels of Alb, and significantly high levels of alanine aminotransferase (ALT). Repopulation of the *h*-hepatocytes in the liver increased the blood Alb concentration and decreased the ALT level, indicating that *h*-hepatocytes contributed to the improvement of *m*-liver function [8]. Based on these considerations and findings, we expect that a *m*-liver made of *h*-hepatocytes would function as an apparently normal liver, metabolizing and detoxifying endogenous and exogenous biomolecules.

4. Expression Profiles of *h*-Cytchrome P450s in Relation to Phase 1 Metabolic Enzymes

Biochemical treatment of foreign substances (xenobiotics) that have been absorbed into the body is one of the major tasks of the liver. In hepatocytes, xenobiotics are processed to more stable and hydrophilic derivatives by groups of enzymes, collectively called xenobiotic-metabolizing enzymes (XMEs), via two phases: phase 1, which is accomplished by oxidative enzyme, and phase 2, performed by conjugating enzymes [17]. Ingested drugs, toxicants, and chemical carcinogens are metabolized in phase I by CYP and the flavin-containing monooxygenase superfamily. Notably, CYP is the key enzyme in the elimination of clinical drugs.

Humans and rodents respond differently to xenobiotics, and this is explained in part by species differences in CYP subfamilies. These species differences raise serious issues in research for clinically usable medicines, because the results of xenobiotic metabolism studies with mice and rats, which are the most commonly used experimental models for pharmacological and toxicological studies, cannot be extrapolated to humans. Thus, information about the expression of CYP families and subfamilies should be valuable from two viewpoints. First, the expression in *h/m*-chimeric mice of

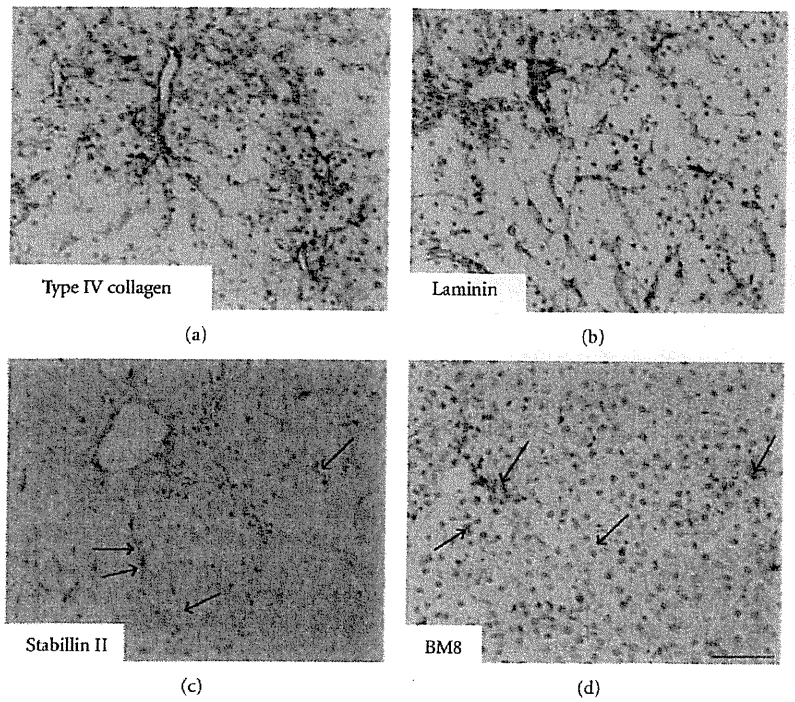

FIGURE 1: The histological harmonization of *h*-hepatocytes with *m*-nonparenchymal cells. uPA/SCID mice were transplanted with *h*-hepatocytes and allowed to grow until the repopulation of the liver was complete. Then, liver sections were prepared from the *h*-hepatocyte-chimeric mice. Sections were immunostained with *m*-specific antibodies for type IV collagen (a); laminin (b); stabillin (c), a marker of liver endothelial cells (a gift from Dr. A. Miyajima, Tokyo University); and BM8 (d), a marker of Kupffer cells. The immunosignals are brown. The arrows in (c) and (d) point to typical immunopositive cells. Bar, 100 μm.

a CYP subtype that is found in *h*-hepatocytes, but not in mice, would be a good indication that the *h*-hepatocytes are biochemically functional in the *m*-iver. Second, the *h*-CYP-expressing chimeric mouse is a useful experimental model for studying *h*-type metabolic responses to xenobiotics, including clinically valuable drugs. Of note, CYP3A4 is the most abundantly expressed CYP in *h*-liver and metabolizes >60% of all therapeutic drugs; collectively, CYP2D6 and CYP3A4 metabolize >70% of the drugs on the market [17].

Species differences in the CYP2C subfamily are well known and have been characterized intensively [18, 19]. The *h*-liver contains four CYP2C isoforms, CYP2C8, CYP2C9, CYP2C18, and CYP2C19, all of which are absent from mice and rats. Western blot analyses using *h*-specific antibodies against CYP2C9 revealed positive signals with hepatocytic microsomal fractions from *h*/*m*-chimeric mice with an RI >34% and from the donor, but not with hepatocytic microsomal fractions from chimeric mice with an RI <28% or from mice that had not been transplanted with *h*-hepatocytes. CYP2C9 catalyzes the 4′-hydroxylation of diclofenac, and the microsomal fractions from the chimeric mice showed diclofenac 4′-hydroxylation activity that depended on the RI of the mouse, strongly suggesting that the *h*-hepatocytes in chimeric livers retain *h*-type pharmacological activity toward drugs. One of the clearest and best-defined examples of a difference in a CYP between mice and humans is CYP2D6 [20, 21], which is involved in the metabolism of a large number of clinically used drugs [22, 23]. In humans, CYP2D6 is the only active member of the CYP2D subfamily, whereas rats and mice do not express a protein with the enzyme activity of *h*-CYP2D6, although they do have at least five other CYP2D genes [20, 24]. The enzymatic activity of *h*-CYP2D6 in the chimeric mouse was demonstrated by orally administering debrisoquin, a *h*-CYP2D6 substrate, to the mice and subsequently detecting 4′-hydroxydebrisoquin, a major debrisoquin metabolite produced by *h*-CYP2D6, in the blood of the mice. Pretreatment of the mice with quinidine, a typical *h*-CYP2D6 inhibitor, decreased the level of the metabolite. Thus, a CYP enzymatic activity in the chimeric mice was specifically induced by a CYP2D6-metabolized drug and specifically suppressed by a CYP2D6 inhibitor [25].

Among the known CYP families, four families (CYP1–4) play primary roles in XMEs. We compared the mRNA and protein expression profiles of six *h*-CYPs, CYP1A1, 1A2, 2C9, 2C19, 2D6, and 3A4, in the chimeric *m*-liver with those in the donor liver [8]. Total RNA was prepared from the livers of chimeric mice with different RIs and of donors, and the mRNA for the six *h*-CYPs was amplified in a quantitative reverse-transcriptase polymerase chain reaction (qRT-PCR).

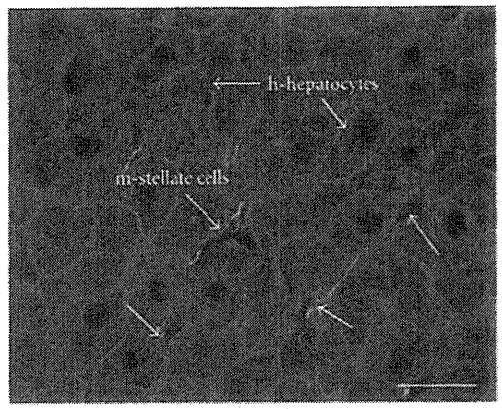

FIGURE 2: Close natural apposition of *m*-stellate cells and *h*-hepatocytes in a chimeric liver. A serial section shown in Figure 1 was doubly stained with *h*-CK8/18 (green) for *h*-hepatocytes and *m*-desmin (orange) for *m*-stellate cells. The *h*-hepatocytes are well organized and closely apposed to *m*-stellate cells in Disse's space. Arrows indicate representative *h*-hepatocytes (green) and *m*-stellate cells (orange). Bar, 10 μm.

All six mRNAs were amplified to detectable levels, which were higher in mice with higher RI values. Thus, the *h*-hepatocytes in the chimeric mice appeared to express the six *h*-CYP genes in a manner similar to their expression in the *h*-body.

We then asked whether these normally expressed *h*-CYPs in the *h*/*m*-chimeric liver were inducible in a drug-specific manner. The *h*-CYP3A4 and *h*-CYP1A subfamilies specifically respond to rifampicin and 3-methylcholanthrene (3-MC), respectively [26]. Chimeric mice with *h*-hepatocytes were injected intraperitoneally with rifampicin or 3-MC, once per day for 4 days. The mRNA levels of the six *h*-CYPs in the liver tissues were measured 24 h after the last injection. Rifampicin treatment enhanced the expression of *h*-CYP3A4 by 5.8-fold, but did not affect the levels of the other five *h*-CYPs. The administration of 3-MC enhanced CYP1A1 and CYP1A2 mRNA levels by 10.0-fold and 6.4-fold, respectively, but had no effect on the other four CYPs. Neither rifampicin nor 3-MC induced the expression of any of the six *h*-CYPs in mice$_{\text{Alb-uPA/SCID}}$ that had not been transplanted with *h*-hepatocytes. Rifabutin, an analogue of rifampicin, also specifically induced *h*-CYP3A, but not the host murine Cyp3a, in the chimeric *m*-liver [27]. The degree of CYP3A4 induction in the chimeric mouse has practical applications in drug testing, because many drugs are CYP3A4 substrates and the induction of CYP3A4 decreases the pharmacological potency of these drugs [17].

Rifampicin is a ligand for the pregnane X receptor (PXR), which forms a heterodimer with retinoid X receptor a (RXRa). Rifampicin/PXR/RXRa subsequently binds to a xenobiotic response element (XRE) composed of the direct repeat of alpha and beta half-sites separated by four nucleotides on the CYP3A4 gene, thereby upregulating its expression in phase I [28]. Rifampicin is a potent activator of human and rabbit PXR, but has little activity in the rat and mouse [29]. Thus, that the liver data of *h*/*m*-chimeric mice faithfully reflect those in humans. The binding of 3-MC to the aryl hydrocarbon receptor (AHR) forms a AHR/3-MC complex, which upregulates CYP1A1, CYP1A2, and CYP1B1 expression by binding, together with the AHR nuclear translocator (ARNT), to the XREs of these genes [30]. Our studies suggest that these known ligand-activated receptor signaling pathways activated by rifampicin and 3-MC are functional in the *h*/*m*-chimeric *m*-liver. Thus, we propose that the hepatocyte-humanized mouse will be a useful animal model in studies of *h*-type signaling pathways that regulate gene expression induced by xenobiotics.

5. Humanization of Phase II Conjugation Pathway of a Drug in *h*/*m*-Chimeric Mice

It is estimated that phase II conjugation accounts for approximately >30% of drug clearance [31], especially of compounds with polar groups. The major hepatic phase II enzymes in humans are UDP-glucuronosyltransferase (UGT), which is responsible for glucuronidation; sulfotransferase (SULT), for sulfation; *N*-acetyltransferase (NAT), for acetylation; and glutathione *S*-transferase (GST), for glutathione conjugation. We examined the mRNA and protein expression and the enzyme activity of the *h*-forms of these enzymes in chimeric mice with livers having RI values ranging from 0 to 90% [32]. The chimeric livers expressed *h*-UGT, *h*-SULT, *h*-NAT, and *h*-GST mRNA and the UGT2B7, SULT1E1, SULT2A1, and GSTA1 proteins at levels that correlated with their RI values. Activities of related enzymes such as morphine 6-glucuronosyltransferase and estrone 3-sulfotransferase were also detected in an RI-dependent manner. The protein content and enzyme activities of phase II-associated enzymes in chimeric *m*-livers with an RI of approximately 90% were similar to those in the donor liver. In a separate study, we systematically compared the mRNA expression profiles for 26 phase II *h*-enzymes, including GST, SUL, NAT, and UGT members, between livers of chimeric mice with RIs of 71–89% and donor livers [16]. All of the tested enzyme genes were detected. For 65% of the tested genes, the expression levels in the chimeric livers were 30 to 55% of the levels in the donor livers; although lower, these values are comparable to the RI values. These results indicate that the hepatic phase II biotransformation of a drug is appreciably humanized in the *h*/*m*-chimeric mouse.

There are groups of drugs in clinical use that bind to PXRs or constitutive androstane receptors (CARs). The ligand-activated PXRs and CARs are involved in the regulation of some phase II XME genes such as SULT1A, UGT1A, and GST [33–35]. Thus, it is likely that these *h*-type ligand-activated transcriptional regulators are functional in *h*/*m*-chimeric *m*-livers, suggesting that these chimeric mice will contribute to studies on the regulation of gene and protein expression of these transcription factors in relation to xenobiotic metabolism.